

THE VIBRATION OF INITIALLY CURVED SIMPLY
SUPPORTED AND CLAMPED BEAMS WITH SLIDING
END MASSES

A thesis presented for the degree of
Master of Engineering

in

Department of Mechanical Engineering
University of Canterbury
Christchurch, NEW ZEALAND

by

YUEMING ZHOU

November 1990

SUMMARY

The object of this study is to investigate the free vibration behaviour of slightly curved simply supported beams and clamped beams connected to axially sliding end masses.

For the simply supported beam, two formulas for the natural frequencies are derived from the theoretical analysis. One is obtained by neglecting the effect of axial inertial force of the beam and the other formula is derived by considering this effect, approximately, using Galerkin's method.

For the clamped beam, an approximate formula is derived using Galerkin's method.

The results of the theoretical analysis of simply supported and clamped beams are described in chapter 2 and show that there are two different natural frequencies having the same fundamental transverse mode for each case and the ratio of the longitudinal motion to transverse motion are different for modes.

In order to verify the theoretical results of simply supported and clamped beams some experiments were conducted. Beams of various curvatures under different end masses are tested in this experimental work. The effects of the beam

curvatures and axial inertial force of the curved simply supported beams on the natural frequencies also were investigated. The results of the experimental analysis of tested beams are described in chapter 3 and are compared with theoretical results in figures in chapter 4.

ACKNOWLEDGEMENT

I wish to express sincere gratitude to Dr. S. Ilanko, whose guidance and supervision have greatly contributed to the completion of this work.

I would also like to thank Professor H. McCallion, Dr. S. Naguleswaran, Mr. Otto Bolt, Mr. K. Brown, Mr. Gary Johson, and all those who helped in the development of this project.

My sincere thanks also go to the technical staff of the Department of Mechanical Engineering who have provided assistance during the execution of this project.

Finally I am deeply grateful to my wife Lingling Cheng for her typing work and encouragement in Christchurch.

NOMENCLATURE

The following list defines the symbols used in this project.

SYMBOL	MEANING
A	Transverse cross sectional area of beam
E	Young's Modulus of aluminium
F	Shear force
I	Second moment of area about the neutral axis of beam
L	Nominal length of the beam (*)
m	Mass per unit length of the beam
M	Weight of the sliding mass
P	Static axial force
P'	Dynamic axial force
r	Radius of gyration
Y_0	Static equilibrium position
Y	Dynamic equilibrium displacement measured from Y_0
Ω_0	Frequency of straight beam
Ω	Frequency of curved beam
Z	Lateral deflection at midspan of beam curvature
u	Dynamic axial displacement
θ	Slope of the curved beam

ϵ	The longitudinal strain
β	Density of the beam
λ_i	The i th natural frequency parameters
Ω_t	Theoretical frequency of the beam
Ω_e	Experimental frequency of the beam

* It is to be noted that the difference between the nominal length and the actual length of slightly curved beam in this project is neglected since the rotations are very small.

CONTENTS

<u>CHAPTER</u>		<u>PAGE</u>
1	Introduction	1
2	Theoretical analysis	5
	2.1 Equation of motion of a slightly curved beam	5
	2.2 Vibration of a slightly curved simply supported beam with axially sliding end masses	11
	2.3 Vibration of a clamped curved beam with axially sliding end masses	14
	2.4 The effect of longitudinal inertia on the vibration of a curved simply supported beams	18
3	Experimental analysis	24
	3.1 Introduction	24
	3.2 Design of the testing equipment	25
4	Results and discussion	38
	4.1 Theoretical results of simply supported beams	38
	4.2 Discussion and comparison of experimental and theoretical results of curved simply supported beams with sliding end masses	43
	4.3 Theoretical results of clamped beams with sliding masses and initial curvature	57

4.4	Discussion and comparison of experimental and theoretical results of clamped beams with sliding end masses	60
4.5	Conclusion	74
4.6	Recommendation for further work	76
<u>REFERENCES</u>		77
Appendix A	Theoretical analysis of the curvature of the simply supported beam	80
Appendix B	The effect of rotary inertia of the end masses	85
Appendix C	Error analysis	89
Appendix D	List of compute programs	92

LIST OF FIGURES

<u>FIGURE</u>	<u>DESCRIPTION</u>	<u>PAGE</u>
2.1.1	Free body diagram of a simply supported beam under lateral vibration	5
2.1.2	Free body diagram of a section of the curved beam subject to dynamic axial tension P'	6

2.2.1	Free body diagram of the end masses of simply supported beam	
2.3.1	Free body diagram of a clamped beam under lateral vibration	14
2.3.2	Free body diagram of the end masses of a clamped beam	15
2.4.1	A small element of curved beam subject to axial dynamic tension P'	18
3.1	Test equipment	37
4.2.1-4.2.8	Frequency(Hz) of simply supported beam vs. end mass(Kg)	46-53
4.2.9	The square of (Ω_t/Ω_0) and (Ω_e/Ω_0) vs. the square of (Z/r) of simply supported beams (12.56x 6.3x600mm beams)	54
4.2.10	The square of (Ω_t/Ω_0) and (Ω_e/Ω_0) vs. the square of (Z/r) of simply supported beams (9.4x3x600mm beams)	55
4.4.1-4.4.8	Frequency(Hz) of clamped beam vs. end masses(Kg)	62-69
4.2.9	The square of (Ω_t/Ω_0) and (Ω_e/Ω_0) vs. the square of (Z/r) of clamped beams (12.56x6.3x600mm beams)	70
4.2.10	The square of (Ω_t/Ω_0) and (Ω_e/Ω_0) vs. the square of (Z/r) clamped beams (9.4x3x600mm beams)	71

LIST OF PHOTOGRAPHS

<u>FIGURE</u>	<u>DESCRIPTION</u>	<u>PAGE</u>
3.1	A setup of testing apparatus	35
3.2	Excitor is set up in longitudinal direction	36

CHAPTER 1 INTRODUCTION

The vibration of the curved beams subject to different boundary support conditions has received considerable attention during recent years since beams are widely used in structures, machines, aircrafts, space vehicles, etc. One of the most commonly used beams in engineering applications is curved beam because there are never perfectly straight beams in applications due to the imperfections caused in manufacture, assembly and gravitational effects if the beams are mounted other than vertically. The effects of above factors are important and several publications have appeared recently in the field of vibration of curved beams with various types of boundary conditions.

Plaut [1] investigated displacement bounds for beam-columns with initial curvature subjected to transient load. Plaut and Johnson [2] studied the effects of initial thrust on the vibration frequencies of a shallow arch with pinned ends. They obtained simple frequency equation, which indicated that the first frequency is dependant on the rise paramant (Z/r). Dickinson [3] studied the lateral vibration of slightly bend slender beam subject to prescribed axial end displacement. He derived the relationships between the induced axial forces and prescribed end displacements, and used them together with an axial load-frequency relationship. Kim [4] studied the

lateral vibration of slightly bent slender beams subject to prescribed axial end displacement. Chi [5] studied linear free vibration of a uniform beam with rotationally restrained ends subject to axial force. Large amplitude free oscillations of beams were analyzed by the Ritz-Galerkin method in reference [6]. Raju [7] used the Rayleigh-Ritz method to study the large amplitude flexural vibration of slender beams and thin plates and Goel studied the free vibration of a beam-mass system with elastically restrained ends.

Some recent publication on experimental work on beam vibration are also worth mentioning. Kim [4] studied the lateral vibration of slightly bent slender beams subject to prescribed axial end displacement. The lower natural frequency corresponding to the first fundamental mode was found by Ling [8]. Bennouna and White [9] studied the effect of large vibration amplitudes on the fundamental mode shape of a clamped-clamped uniform beam, and expressed their results on the fundamental resonance frequency as a function of the amplitude to beam thickness ratio. The importance of rotational boundary conditions was experimentally investigated by Picard [10].

The vibration behaviour of simply supported and clamped curved beams with sliding end masses, which correspond to the first and second fundamental modes have not been experimentally investigated in the literature, and so have the effects of axial inertial

force of the beam on the natural frequency.

In present work, the natural frequencies and mode shapes of slightly curved beam with sliding end masses subject to different boundary support conditions are studied. The emphasis of this project is on the natural frequencies which correspond to fundamental transverse modes. A series of investigations are carried out in order to achieve good agreement between the theoretical and experimental results. A computer program capable of solving the complex frequency equation which considers axial inertia of the simply supported beam and another program capable of calculating the natural frequencies of clamped beam have been developed for this project.

The development of this project is separated into two stages, theoretical and experimental analysis.

In the theoretical analysis, Galerkin's method is used to derive frequency equations of both simply supported and clamped beams. The results of theoretical analysis of simply supported and clamped beams show that for a given value of end mass, there are two different natural frequencies corresponding to fundamental transverse modes and the ratio of the longitudinal motion to transverse motion are different for modes. They also show that the natural frequencies of the beams having various rise parameters are dependant on the boundary conditions. This is very significant particularly for the second fundamental modes.

In order to assess the applicability of theoretical analysis, an experimental analysis was conducted. A multiple test equipment is designed, which could be used to measure and record the natural frequencies of the beam and could be changed into different boundary conditions to meet different requirements. In contrast to previous experimental work, the effect of exciting direction has been taken into account in the design, so that the modes having significant axial motion may be picked up. The excitor which is used to excite test beams in both transverse and longitudinal directions was held in an adjustable device Fig(3.1) to meet different requirements.

The results of experimental and theoretical analysis of both simply supported and clamped beams are compared graphically and are tabled in chapter 4. The experimental set up and test procedures are described in chapter 3. The curvature of tested beam are taken as Fourier series to model real shape and the effect of inertial force of the clamped beam with sliding end mass are given appendix A.

Although results show there are some considerable discrepancies between the experimental and theoretical results for the beams with large initial curvatures, the agreement achieved for the beams having small initial curvature is encouraging. Besides the presence of two different natural frequencies and modes having the same transverse deflection form has been established theoretically and experimentally.

CHAPTER 2
THEORETICAL ANALYSIS

2.1 EQUATION OF MOTION OF A SLIGHTLY CURVED BEAM

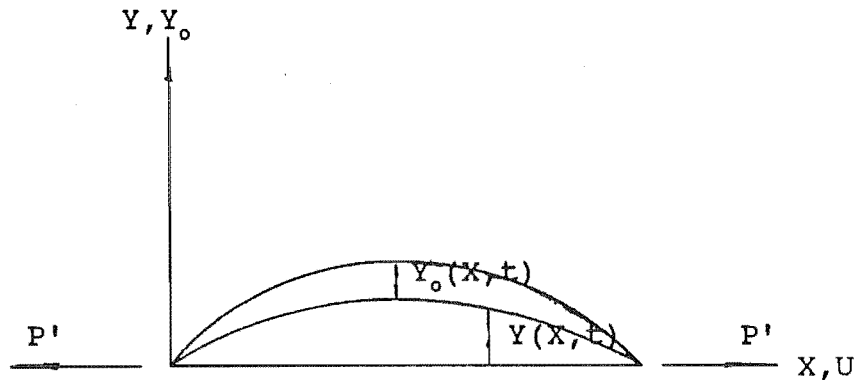
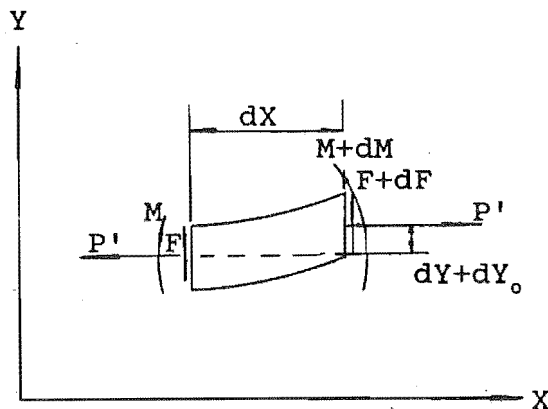


Figure (2.1.1) Free body diagram of a simply supported beam under lateral vibration.

The analysis is done by considering a uniform curved beam with length L , cross sectional area A , second moment of area I , young modulus E , initial displacement $Y(x, t)$, dynamic equilibrium displacement $Y_0(x, t)$ measured from $Y(x, t)$ and dynamic axial tension induced during the vibration p' (See Figure 2.1.1).

In the analysis, it is assumed that the free transverse vibration is in plane; that the amplitudes of deflection of beam during vibration are small compared to the wave length of the vibration; that the depth of the beam is small compared

with its radius of curvature and its maximum displacement; that the plane section remains plane at all phases of an oscillation; that the deformation due to shearing of one cross section relative to an adjacent one is negligible. In addition, one should assume that one principle axial of a typical cross-section is perpendicular to the direction of motion in the vibration; and that its mass is concentrated at its neutral axis.



Figure(2.1.2) Free body diagram of a section of the curved beam subject to dynamic axial tension p' .

Considering a small section of the beam, dx subject to dynamic axial tension p' . Let m be the mass per unit length. Applying Newton's second law in Y-direction;

$$dF = m dx \frac{\partial y^2}{\partial t^2}$$

Neglecting the rotary inertia of the beam, for rotational equilibrium, taking a moment

$$M - (M + dM) - FdX + P(dY_0 + dY) = 0$$

$$-dM - FdX + P'(dY_0 + dY) = 0$$

$$F = -dM/dX + P'(dY_0 + dY)/dX$$

As $dX \rightarrow 0$

$$F = - \frac{dM}{dX} + \frac{P'(dY_0 + dY)}{dX}$$

$$dF = \frac{\partial F}{\partial X} dX$$

$$= \left[- \frac{\partial^2 M}{\partial X^2} + P' \left(\frac{\partial^2 Y_0}{\partial X^2} + \frac{\partial^2 Y}{\partial X^2} \right) \right] dX$$

but $dF = (m dX) \partial^2 Y / t^2$

Therefore

$$m dX \frac{\partial^2 Y}{\partial t^2} + \left[\frac{\partial^2 M}{\partial X^2} - P' \left(\frac{\partial^2 Y_0}{\partial X^2} + \frac{\partial^2 Y}{\partial X^2} \right) \right] dX = 0$$

$$m \frac{\partial^2 Y}{\partial X^2} + \frac{\partial^2 M}{\partial X^2} - P' \left(\frac{\partial^2 Y_0}{\partial X^2} + \frac{\partial^2 Y}{\partial X^2} \right) = 0$$

Substituting the beam bending formula $M = E \partial^2 Y / \partial X^2$ into the above equation gives

$$EI \frac{\partial^4 Y}{\partial X^4} - P' \left(\frac{\partial^2 Y_0}{\partial X^2} + \frac{\partial^2 Y}{\partial X^2} \right) + m \frac{\partial^2 Y}{\partial t^2} = 0$$

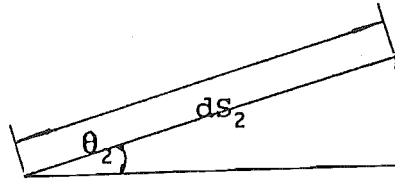
As $Y \ll Y_0$, the partial differential equation governing the motion of a curved beam is

$$EI \frac{\partial^4 Y}{\partial X^4} - P' \frac{\partial^2 Y_0}{\partial X^2} + m \frac{\partial^2 Y}{\partial t^2} = 0 \quad (2.1.1)$$

The longitudinal strain ϵ results from longitudinal and transverse motion of the beam. The strain due to longitudinal motion is given by $\epsilon_0 = \partial u / \partial X$. Where u is dynamic axial displacement of the beam. The strain due to transverse motion is found by considering the geometry of a deflected element of the beam.

Considering a small section of the beam dS , let θ be the slope of the curved beam, then as a result of transverse motion the slope changes from

$$\theta_1 = dY_0/dX \longrightarrow \theta_2 = dY_0/dX + dY/dX$$



At maximum excursion, changing in dS_2

$$\begin{aligned} \delta S_{\max} &= dS_2 - \cos\theta_2 \\ &= dS_2(1 - \cos\theta_2) \end{aligned}$$

Using Taylor's expansion, for a small θ ,

$$\cos\theta \approx 1 - \theta^2/2$$

$$\begin{aligned} \delta S_{\max} &= dS_2 \theta_2^2 / 2 \\ &= \frac{dS_2}{2} \left(\frac{dY_0 + dY}{dX} \right)^2 \end{aligned}$$

$$\begin{aligned} \epsilon_{\max} &= \delta S_{\max} / dS \\ &= \theta^2 / 2 \\ &= (dY_0/dX + dY/dX)^2 / 2 \end{aligned}$$

At equilibrium position

$$\delta S_1 = dS_1 (1 - \cos \theta_1)$$

$$\theta_1 = dY_0 / dX$$

Using Taylor's expansion

$$\epsilon_1 = \delta S_1 / dS_1$$

$$= \theta_1^2 / 2$$

$$= (dY_0 / dX)^2 / 2$$

For a initial curved beam, changing in strain ϵ

$$\epsilon = \epsilon_{\max} - \epsilon_1$$

$$= (\partial Y / \partial X + \partial Y_0 / \partial X)^2 / 2 - (\partial Y_0 / \partial X)^2 / 2$$

$$= (\partial Y / \partial X)^2 / 2 + (\partial Y / \partial X) (\partial Y_0 / \partial X)$$

As $Y_0 \gg Y$, $\epsilon \approx (\partial Y / \partial X) (\partial Y_0 / \partial X)$

Thus total dynamic strain (ϵ_t)

$$\epsilon_t = \partial u / \partial X + (\partial Y / \partial X) (\partial Y_0 / \partial X)$$

But $P' = EA \epsilon_t$

Therefore total dynamic force

$$P' = EA \left(\frac{\partial u}{\partial X} + \frac{\partial Y}{\partial X} \frac{\partial Y_0}{\partial X} \right) \quad (2.1.2)$$

Neglecting the axial inertial force fo the beam,

$$\frac{\partial P'}{\partial X} = 0$$

$$\frac{\partial^2 u}{\partial X^2} + \frac{\partial}{\partial X} \left(\frac{\partial Y_0}{\partial X} \frac{\partial Y}{\partial X} \right) = 0$$

Rearranging equation (2.1.2)

$$\frac{P'}{EA} = \frac{\partial u}{\partial X} + \frac{\partial Y_0}{\partial X} \frac{\partial Y}{\partial X}$$

$$\frac{\partial u}{\partial X} = \frac{P'}{EA} - \frac{\partial Y_o \partial Y}{\partial X \partial X}$$

Integrating,

$$u = \int \left(\frac{P'}{EA} - \frac{\partial Y_o \partial Y}{\partial X \partial X} \right) dX + D$$

$$u = \frac{P'X}{EA} - \int \left(\frac{\partial Y_o \partial Y}{\partial X \partial X} \right) dX + D \quad (2.1.3)$$

Where D is constant of integration.

Substitution of the two axial end conditions into the above equation would lead to an expression for the integration, constant D, as explained later.

2.2 VIBRATION OF A SIMPLY SUPPORTED CURVED BEAM WITH AXIALLY SLIDING MASSES

Now consider the vibration of a simply supported beam with sliding end masses as shown in Figure (2.2.1) The transverse boundary conditions would be satisfied if it is assumed that:

$$(1) \quad Y_0(X,t) = Z \sin(\pi X/L) \quad (2.2.1)$$

$$(2) \quad Y(X,t) = C \sin(\pi X/L) \quad (2.2.2)$$

These shapes are chosen because they correspond to the fundamental natural frequency mode of vibration which is investigated in this study.

Substituting these into equation (2.1.3) gives,

$$u(X) = P'(X)/(EA) - (1/2) ZC(\pi/L)^2 [L \sin(\pi X/L) + X] + D \quad (2.2.3)$$

Where D is an integration constant.

Considering the boundary condition of sliding end mass at both sides:

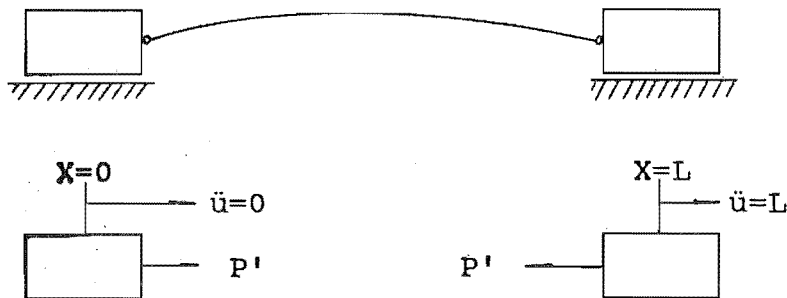


Figure (2.2.1) Free body diagram of the end masses of simply supported beam

Assuming the motion to be simple harmonic,

$$\ddot{u}(x) + \Omega^2 u(x) = 0$$

At $X=0$

$$\partial^2 u(0) / \partial t^2 = -\Omega^2 u(0)$$

Applying Newton's 2nd law to the sliding mass at $x=0$ gives:

$$P' = M[-\Omega^2 u(0)] \quad (2.2.4)$$

Substituting equation (2.2.3) into equation (2.2.4) gives:

$$D = P' / M\Omega^2 \quad (2.2.5)$$

Similarly at $X=L$,

$$-P' = M\partial^2 u(L) / \partial t^2 = -M\Omega^2 u(L) \quad (2.2.6)$$

Substituting equation (2.2.3) into equation (2.2.4)

$$P' = M\Omega^2 \left[\frac{P'L}{EA} - \left(\frac{2\pi ZC}{2L} + \frac{P'}{M\Omega^2} \right) \right]$$

Rearranging,

$$P' = - \frac{M\Omega^2 \pi^2 ZC}{2L(2 - M\Omega^2 L / EA)} \quad (2.2.7)$$

Substituting equations (2.2.1) and (2.2.2) into equation (2.1.1) and using $\partial^2 Y / \partial t^2 = -\Omega^2 Y$ gives,

$$EI\pi^4 C \sin(\pi X/L) / L^4 + P'\pi^2 Z \sin(\pi X/L) / L^2 - m\Omega^2 C \sin(\pi X/L) = 0 \quad (2.2.8)$$

For non-trivial solution,

$$\frac{EI\pi^4}{mL^4} - \frac{Z^2\pi^4}{2mL^4} \left(\frac{EAM\Omega^2 L}{2EA - M\Omega^2 L} \right) = \Omega^2 \quad (2.2.9)$$

Fundamental frequency of a simply supported beam

without axial loading and initial curvature is as follows:

$$\Omega_0 = \frac{\pi^2}{L^2} \left(\frac{EI}{m} \right)^{0.5}$$

Radius of gyration r is

$$r = \sqrt{I/A}$$

Substituting these into equation (2.2.9) yields:

$$\Omega^2 = \Omega_0^2 - \frac{\Omega_0 Z}{2r^2} \left(\frac{M\Omega^2 L}{2EA - M\Omega^2 L} \right)$$

Rearranging

$$\frac{\Omega^2}{\Omega_0^2} = 1 + \frac{Z^2}{2r^2} \left(\frac{M\Omega^2 L}{2EA - M\Omega^2 L} \right) \quad (2.2.10)$$

Equation (2.2.10) represents the equation for the natural frequency of an initially curved simply supported uniform beam with two equal axially sliding end masses neglecting axial inertia of the beam. In chapter 3, an experimental investigation carried out to verify this equation is described.

2.3 VIBRATION OF A CLAMPED CURVED BEAM WITH AXIALLY SLIDING END MASS

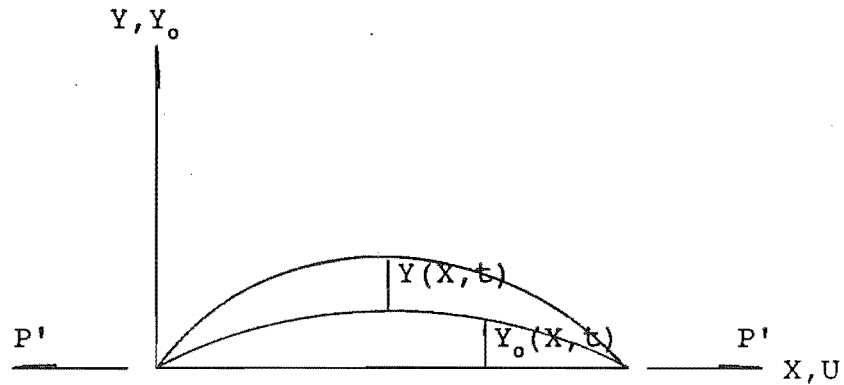


Figure (2.3.1) Free body diagram of a clamped beam under lateral vibration.

Let the initial shape of the beam Y' be given by

$$Y_0 = Z[1 - \cos(2\pi X/L)] \quad (2.3.1)$$

This would satisfy the transverse geometrical boundary conditions. The transverse dynamic displacement $Y(X)$ of the beam measured from the equilibrium position $Y_0(X)$, may also be given as

$$Y(X) = C[1 - \cos(2\pi X/L)] \quad (2.3.2)$$

The curved beam vibration equation for harmonic motion is

$$EI \frac{\partial^4 Y}{\partial X^4} - P' \frac{\partial^2 Y}{\partial X^2} - m\Omega^2 Y = 0 \quad (2.3.3)$$

Substituting equation (2.3.1) and (2.3.2) into equation

(2.1.3) gives:

$$u(X) = \frac{P'X}{EA} - \frac{2\pi ZC}{L} \left(\frac{\pi X}{L} - \frac{1}{4} \sin \frac{4\pi X}{L} + D \right) \quad (2.3.4)$$

Where D is a constant of integration.

Considering the boundary condition of the sliding end mass at both sides.

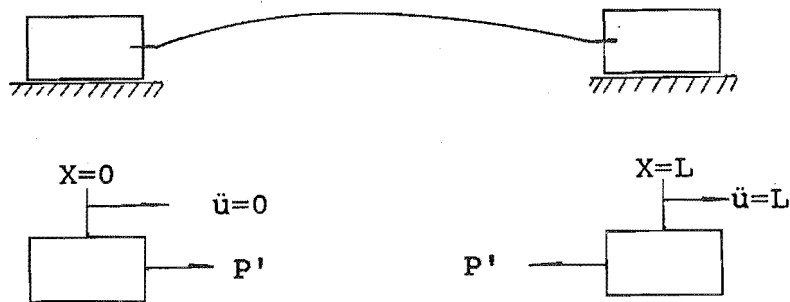


Figure (2.3.2) Free body diagram of the end masses of a clamped beam.

At $X=0$

$$\frac{\partial^2 u(0)}{\partial t^2} = -\Omega^2 u(0)$$

$$P' = M[-\Omega^2 u(0)] \quad (2.3.5)$$

Substituting equation (2.3.4) into equation (2.3.3)

$$u(0) = -2\pi ZCD/L$$

$$P' = M\Omega^2 2\pi ZCD/L$$

$$D = P'L / (M\Omega^2 2\pi ZC)$$

At $X=L$

$$-P = M\frac{\partial^2 u(L)}{\partial X^2} = -M\Omega^2 u(L) \quad (2.3.6)$$

Substituting equation (2.3.4) into equation (2.3.6)

As

$$u(L) = \frac{P'X}{EA} - \frac{2\pi ZC}{L} \left(\pi + \frac{P'L}{M\Omega^2 2\pi X C} \right)$$

$$P' = M\Omega^2 (P'L/EA - 2\pi^2 ZC/L - P'/M\Omega^2)$$

$$P' = - \frac{2M\Omega^2 \pi^2 ZC}{L(2 - M\Omega^2 L/EA)} \quad (2.3.7)$$

To substitute equation (2.3.7) into equation (2.3.3)

$$\text{As } \partial^2 Y / \partial X^2 = Z(4\pi^2/L^2) \cos(2\pi X/L)$$

$$\partial^4 Y / \partial X^4 = -C(16\pi^4/L^4) \cos(2\pi X/L)$$

$$EIC(2\pi/L)^4 \cos(2\pi X/L) + P'Z(2\pi/L)^2 \cos(2\pi X/L) + m\Omega^2 C[1 - \cos(2\pi X/L)] = 0$$

$$EI \frac{16\pi^4}{L^4} \cos(2\pi X/L) - \frac{8Z^2 \pi^4 M}{L^3(2 - M\Omega^2 L/EA)} \cos(2\pi X/L) + m\Omega^2 -$$

$$m\Omega^2 \cos(2\pi X/L) = 0 \quad (2.3.8)$$

Applying Galerkin's method to equation (2.3.8) using $W = 1 - [\cos(2\pi X/L)]$ as the weighting function. Let:

$$F(X, t) = EI \frac{16\pi^4}{L^4} \cos(2\pi X/L) - \frac{8Z^2 \pi^4 M\Omega^2}{L^3(2 - M\Omega^2 L/EA)} \cos(2\pi X/L) + m\Omega^2 -$$

$$m\Omega^2 \cos(2\pi X/L)$$

$$\text{Then } \int_0^1 F(X, t) W \, dX = 0$$

$$\text{ie. } \int_0^1 \left[EI \frac{16\pi^4}{L^4} \cos(2\pi X/L) - \frac{8Z^2 \pi^4 M\Omega^2}{L^3(2 - M\Omega^2 L/EA)} \cos(2\pi X/L) + m\Omega^2 - \right.$$

$$\left. m\Omega^2 \cos(2\pi X/L) \right] [1 - \cos(2\pi X/L)] \, dX = 0$$

$$\frac{3mL}{2} \Omega^2 + \frac{4Z^2 \pi^4 M\Omega^2}{(2 - M\Omega^2 L/EA)} - EI \frac{8\pi^2}{L^3} = 0 \quad (2.3.9)$$

Equation (2.3.9) represents the equation for the natural frequency of an initially curved clamped beam with two, equal, axially sliding masses.

2.4 THE EFFECT OF LONGITUDINAL INERTIA ON THE VIBRATION OF A CURVED SIMPLY SUPPORTED BEAM

As there were discrepancies between the experimental results and the theoretical results obtained in section 2.2, it was decided to investigate the influence of longitudinal inertia of the beam. This was done by solving the beam vibration equation including longitudinal inertia using Galerkin's method. This approximate analysis is described below:

Considering the axial motion of an element of the curved beam as shown in Figure(2.4.1)

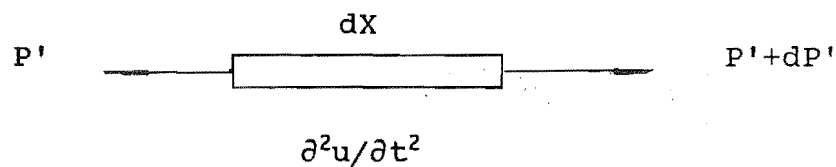


Figure (2.4.1) A small element of curved beam subject to dynamic axial tension p' .

From Newton's second law:

$$dP' = A\beta \cdot dx \frac{\partial^2 u}{\partial t^2} \quad (2.4.1)$$

But for simple harmonic motion,

$$\frac{\partial^2 u(x)}{\partial t^2} + u\Omega^2 = 0$$

Therefore,

$$\frac{\partial P'}{\partial X} = -\beta A \Omega^2 u \quad (2.4.2)$$

From equation (2.1.2)

$$P' = EA \left(\frac{\partial u}{\partial X} + \frac{\partial Y}{\partial X} \frac{\partial Y_0}{\partial X} \right)$$

Using equations (2.2.1) and (2.2.2) for Y and Y₀ of a simply supported beam

$$\begin{aligned} \frac{\partial P'}{\partial X} &= EA \partial^2 u / \partial X^2 - 2CZ (\pi/L)^3 \cos(\pi X/L) \sin(\pi X/L) \\ &= EA \partial^2 u / \partial X^2 - CZ (\pi/L)^3 \sin(2\pi X/L) \end{aligned} \quad (2.4.3)$$

From equations (2.4.2) and (2.4.3)

$$EA \partial^2 u / \partial X^2 - CZ (\pi/L)^3 \sin(2\pi X/L) \cdot EA + \beta A \Omega^2 u(x) = 0$$

Rearranging

$$\partial^2 u / \partial X^2 + (\beta/E) \Omega^2 u(x) = CZ (\pi/L)^3 \sin(2\pi X/L)$$

Let $(\beta/E) \Omega^2 = K^2$ and $B = CZ (\pi/L)^3$ gives:

$$\partial^2 u / \partial X^2 + K^2 u = B \sin(2\pi X/L) \quad (2.4.4)$$

The solution of equation (2.4.4) may taken as follows:

$$u(x) = \sum D_j \sin(j\pi X/L) + G_1 X + G_2 \quad (2.4.5)$$

$$\partial^2 u / \partial X^2 = -\sum (j/L)^2 D_j \sin(j\pi X/L) \quad (2.4.6)$$

$$K^2 u = \sum K^2 D_j \sin(j\pi X/L) + G_1 X + G_2 \quad (2.4.7)$$

Substituting equations (2.4.6) and (2.4.7) into equation (2.4.4)

$$\Sigma [K^2 - (j\pi/L)^2] D_j \sin(j\pi X/L) + (G_1 X + G_2) K^2 = B \sin(2\pi X/L) \quad (2.4.8)$$

Applying Galerker's method to solve equation(2.4.8)

Using $\sin(l\pi X/L)$ as the weighting function.

$$\begin{aligned} & \int_0^1 (\Sigma[K^2-(j\pi/L)^2]D_j \sin(j\pi X/L) + (G_1 X + G_2) K^2) \sin(l\pi X/L) \, dX \\ &= \int_0^1 B \sin(2\pi X/L) \sin(l\pi X/L) \, dX \\ & \int_0^1 \Sigma[K^2-(j\pi/L)^2]D_j \sin(j\pi X/L) \sin(l\pi X/L) \, dX \\ &+ \int_0^1 (G_1 X + G_2) K^2 \sin(l\pi X/L) \, dX = \int_0^1 B \sin(2\pi X/L) \sin(l\pi X/L) \, dX \end{aligned} \quad (2.4.9)$$

Taking only one term in the series, with $j=l=2$,

since $\int_0^1 \sin^2(2\pi X/L) \, dX = L/2$, equation(2.4.9) becomes:

$$\begin{aligned} & \frac{L}{2} \left(K^2 - \frac{4\pi^2}{L^2} \right) D_2 - K^2 G_1 \frac{L^2}{2\pi} - \frac{BL}{2} \\ & D_2 = (B + K^2 G_1 L / \pi) / (K^2 - 4\pi^2 / L^2) \end{aligned} \quad (2.4.10)$$

Substituting equation(2.4.10) into equation(2.4.5)

gives:

$$u = \frac{(B + K^2 G_1 L / \pi)}{K^2 - 4\pi^2 / L^2} \sin(2\pi X/L) + G_1 X + G_2 \quad (2.4.11)$$

From equation(2.1.2)

$$\begin{aligned} \frac{\partial u}{\partial X} &= \frac{P'}{EA} - \frac{\partial Y_0 \partial Y}{\partial X \partial X} \\ &= \frac{P'}{EA} - CZ (\pi/L)^2 \cos^2(2\pi X/L) \end{aligned} \quad (2.4.12)$$

Considering the longitudinal boundary condition of the simply supported beam, as section 2.2,

$$P'(0) = -M\Omega^2 u(0) \quad (2.4.13)$$

$$P'(L) = M\Omega^2 u(L) \quad (2.4.14)$$

Differentiating equation(2.4.11) gives:

$$\partial u / \partial X = \frac{(B + K^2 G_1 L / \pi)}{K^2 - 4\pi^2 / L^2} \cos(2\pi X / L) + G_1 \quad (2.4.15)$$

From this

$$\partial u(0) / \partial X = \partial u(L) / \partial X = \frac{2\pi(B + K^2 G_1 L / \pi)}{L(K^2 - 4\pi^2 / L^2)} + G_1 \quad (2.4.16)$$

From equations(2.4.11), (2.4.12) and (2.4.13)

$$\partial u(0) / \partial X = -M\Omega^2 G / EA - CZ\pi^2 / L^2 \quad (2.4.17)$$

$$\partial u(L) / \partial X = (M\Omega^2 / EA) (G_1 L + G_2) - CZ\pi^2 / L^2 \quad (2.4.18)$$

From equation(2.4.16), $\partial u(0) / \partial X = \partial u(L) / \partial X$,

$$G_1 L + 2G_2 = 0, \quad G_2 = -LG_1 / 2 \quad (2.4.19)$$

From equations(2.4.16), (2.4.17) and (2.4.19)

$$\frac{LM\Omega^2 G_1}{2EA} - \frac{\pi^2}{L^2} = G_1 + \frac{2\pi B}{L(K^2 - 4\pi^2 / L^2)} + \frac{2G_1 K^2}{K^2 - 4\pi^2 / L^2}$$

$$G_1 = \frac{-CZ\pi^2 / L^2 - 2\pi B / (K^2 - 4\pi^2 / L^2)}{1 + 2K^2 / (K^2 - 4\pi^2 / L^2) - M\Omega^2 L / (2EA)} \quad (2.4.20)$$

Substituting equation(2.4.20) and $B = CZ\pi / L$ into equation(2.3.16)

$$\partial u / \partial X = \frac{-CZ\pi^2 / L^2 - 2\pi B / (K^2 - 4\pi^2 / L^2)}{1 + 2K^2 / (K^2 - 4\pi^2 / L^2) - M\Omega^2 L / (2EA)} + \frac{2\pi \cos^2(2\pi X / L)}{L(K^2 - 4\pi^2 / L^2)}$$

$$CZ\pi^3 / L^3 + \frac{-CZ\pi^2 / L^2 - 2\pi B / (K^2 - 4\pi^2 / L^2)}{1 + 2K^2 / (K^2 - 4\pi^2 / L^2) - M\Omega^2 L / (2EA)} K^2 \quad (2.4.20)$$

Substituting equation(2.3.22) into equation(2.1.2)

$$P' = EA \left(\frac{\partial u}{\partial X} + \frac{\partial Y}{\partial X} \frac{\partial Y_0}{\partial X} \right)$$

$$=EA \left(\frac{-CZ\pi^2/L^2 - 2\pi B/(K^2-4\pi^2/L^2)}{1+2K^2/(K^2-4\pi^2/L^2) - M\Omega^2 L/(2EA)} + \frac{2\pi \cos(2\pi X/L)}{L(K^2-4\pi^2/L^2)} \right) [$$

$$CZ\pi^3/L^3 + \frac{-CZ\pi^2/L^2 - 2\pi B/(K^2-4\pi^2/L^2)}{1+2K^2/(K^2-4\pi^2/L^2) - M\Omega^2 L/(2EA)} K^2] +$$

$$EACZ \frac{\pi^2}{L^2} \cos^2(\pi X/L)$$

$$P' = EACZ \frac{\pi^2}{L^2} \left(\frac{-CZ\pi^2/L^2 - 2\pi B/(K^2-4\pi^2/L^2)}{1+2K^2/(K^2-4\pi^2/L^2) - M\Omega^2 L/(2EA)} + \frac{2\pi \cos(2\pi X/L)}{L(K^2-4\pi^2/L^2)} \right) [$$

$$CZ\pi^3/L^3 + \frac{-CZ\pi^2/L^2 - 2\pi B/(K^2-4\pi^2/L^2)}{1+2K^2/(K^2-4\pi^2/L^2) - M\Omega^2 L/(2EA)} K^2] +$$

$$EACZ \frac{\pi^2}{L^2} \cos^2(\pi X/L)$$

$$P' = EACZ \frac{\pi^2}{L^2} \left(\frac{-1 - 2\pi^2/[L^2(K^2-4\pi^2/L^2)]}{1+2K^2/(K^2-4\pi^2/L^2) - M\Omega^2 L/(2EA)} + \frac{2\cos(2\pi X/L)}{(K^2-4\pi^2/L^2)} \right) [$$

$$\pi^2/L^2 + \frac{-CZ\pi^2/L^2 - 2\pi B/(K^2-4\pi^2/L^2)}{1+2K^2/(K^2-4\pi^2/L^2) - M\Omega^2 L/(2EA)} K^2] + \cos^2(\pi X/L)$$

$$(2.4.22)$$

Substituting equation(2.3.22) into equation(2.1.11)

$$EI\partial^4 Y/\partial X^4 - P'\partial^2 Y/\partial X^2 - m\Omega^2 Y = 0$$

$$EI \frac{\partial^4 Y}{\partial X^4} - EACZ \frac{\pi^2}{L^2} \left(\frac{-1 - 2\pi^2/[L^2(K^2-4\pi^2/L^2)]}{1+2K^2/(K^2-4\pi^2/L^2) - M\Omega^2 L/(2EA)} + \frac{2\cos(2\pi X/L)}{(K^2-4\pi^2/L^2)} \right) [$$

$$\pi^2/L^2 + \frac{-CZ\pi^2/L^2 - 2\pi B/(K^2-4\pi^2/L^2)}{1+2K^2/(K^2-4\pi^2/L^2) - M\Omega^2 L/(2EA)} K^2]$$

$$+ \cos^2(\pi X/L) \partial^2 Y/\partial X^2 - m\Omega^2 Y = 0 \quad (2.4.23)$$

Applying Galerkin's method to equation(2.4.23) using

$W = \sin(\pi X/L)$ as a weighting function:

$$\int_0^1 EI C \frac{\pi^4}{L^4} \sin^2(\pi X/L) dx - \int_0^1 EACZ \frac{\pi^4}{L^4} \left(\frac{-1 - 2\pi^2/[L^2(K^2-4\pi^2/L^2)]}{1+2K^2/(K^2-4\pi^2/L^2) - M\Omega^2 L/(2EA)} + \right.$$

$$\left. \frac{2\cos(2\pi X/L)}{K^2-4\pi^2/L^2} \right) [\pi^2/L^2 + \frac{-CZ\pi^2/L^2 - 2\pi B/(K^2-4\pi^2/L^2)}{1+2K^2/(K^2-4\pi^2/L^2) - M\Omega^2 L/(2EA)} K^2]$$

$$+\cos^2(\pi X/L) \sin^2(\pi X/L) dX - m\Omega^2 c \int_0^L \sin^2(\pi X/L) dX = 0 \quad (2.4.24)$$

Since:

$$\int_0^L \sin^2(\pi X/L) dX = L/2, \quad \int_0^L \cos(2\pi X/L) \sin^2(\pi X/L) dX = -L/4$$

$$\text{and } \int_0^L \cos^2(\pi X/L) \sin^2(\pi X/L) dX = L/8,$$

Equation(2.4.24) becomes:

$$EI \frac{\pi^4}{2L^3} + EAZ^2 \frac{\pi^4}{2L^3} \left\{ \frac{-1 - 2\pi^2/[L^2(K^2 - 4\pi^2/L^2)]}{1 + 2K^2/(K^2 - 4\pi^2/L^2) - M\Omega^2 L/(2EA)} - \right.$$

$$\left. \frac{1}{K^2 - 4\pi^2/L^2} \left[\pi^2/L^2 + \frac{-CZ\pi^2/L^2 - 2\pi B/(K^2 - 4\pi^2/L^2)}{1 + 2K^2/(K^2 - 4\pi^2/L^2) - M\Omega^2 L/(2EA)} K^2 \right] \right.$$

$$\left. + 1/4 \right\} - m\Omega^2 L/2 = 0$$

Rearranging:

$$EI \frac{\pi^4}{L^3} + EAZ^2 \frac{\pi^4}{L^3} \left\{ \frac{-1 - 2\pi^2/[L^2(K^2 - 4\pi^2/L^2)]}{1 + 2K^2/(K^2 - 4\pi^2/L^2) - M\Omega^2 L/(2EA)} - \right.$$

$$\left. \frac{1}{K^2 - 4\pi^2/L^2} \left[\pi^2/L^2 + \frac{-CZ\pi^2/L^2 - 2\pi B/(K^2 - 4\pi^2/L^2)}{1 + 2K^2/(K^2 - 4\pi^2/L^2) - M\Omega^2 L/(2EA)} K^2 \right] \right.$$

$$\left. + 1/4 \right\} - m\Omega^2 = 0 \quad (2.4.25)$$

Equation(2.4.25) represents the equation for the natural frequency of an initially curved simply supported beam calculated by considering the effect of initial force of the beam. An experimental investigation was carried out to verify the formulas derived in this chapter. The description of these experiments is given in the next chapter.

CHAPTER 3 EXPERIMENTAL ANALYSIS

3.1 INTRODUCTION OF EXPERIMENTS

The object of the experiments was to measure the natural frequencies of the beams subject to different boundary conditions. An interesting point to note is the presence of two different natural frequencies corresponding to the fundamental mode of a beam. The lower one and higher one were named first and second fundamental natural frequency in this report. For example, the curved simply supported beams with axial sliding end masses have two different natural frequencies, for transverse mode having one half sine wave. The ratios of the longitudinal motion to the transverse motion are different for these modes as discussed in chapter 5.

Providing the boundary conditions that can be accurately and conveniently modelled in the theoretical analysis was a major task in the design of the experimental apparatus, so a multiple testing apparatus was designed as described in section 3.1.2. A set up of testing apparatus for measuring the natural frequency of a beam was shown in Photograph(3.1).

The test rig was designed to test beams with two different transverse boundary conditions. The support blocks

could be used to provide either "simply supported" or "clamped" boundary conditions.

3.2 DESIGN OF THE TESTING EQUIPMENT

The design of the testing equipment was governed by the following requirements:

(1) to hold the beam in a suitable position with respect to the excitor which could be used to excite the beams axially and laterally.

(2) to satisfy different boundary support conditions of the beams in both lateral and longitudinal directions.

3.2.1 CHASSIS

The chassis frame shown in (Figure 3.1 No.9) was made up of two main steel channels of dimensions 120 X 50 X 1600mm welded together to form a rigid support. This setup was expected to support the end blocks and additional masses Figure(3.1) effectively and to prevent any lateral motions of the ends of the beams.

3.2.2 FIXED BASES AND SLIDING BLOCKS

For the boundary condition of clamped and simply supported beam with the sliding end masses, the axial motion between the fixed base and sliding block was expected to be very small. A provision was made (but not used in this project) for the boundary condition of simply supported and clamped beams with lateral elastic support and sliding end masses. In order to minimize friction against axial motion of sliding masses, five bearings ball were used, four in the machined grooves of the fixed bases and sliding blocks, another one in the machined groove of sliding block and the flat surface of adjusting screw I (Figure 3.1). The adjusting screw I was expected to provide a axial moving orbit in the bottom of the sliding block and could be adjusted to change the gap of bearing balls, so that the sliding blocks could be made move freely in axial direction. since the balls could roll along the "V" grooves, some grease was applied to the ball bearing to minimize the friction. Also, the method of heat treatment was applied to make V-grooves and the flat surface of the adjusting screw hard enough to resist abrasion due to weights which was ranged up to 45 Kg.

The adjusting screw and sliding block was designed to satisfy the boundary conditions of the beams with sliding mass and lateral elastic-support (Figure 3.1). The

adjusting screw had a thin elastic steel bar in the middle to provide a lateral support to the sliding masses. A longer screw was also made to make the supports flexible in the lateral direction. In this case, the elastic displacement of the adjusting screw during the vibration was very small compared to the gap between the sliding block and fixed base, the contribution of the displacement was neglected. This was however, not used in the experiments.

The two bolts were used in the fixed base (Figure 3.1. B1) to clamp the sliding end masses to test the beams under axially restrained condition corresponding to attaching infinite end masses.

3.2.3 SUPPORT OF THE BEAMS

In order to satisfy different boundary condition of the beam, fixed supports I,II were used for clamped beams, simple support I was used for simply supported beams with pin joint and simple support II which has V-grooves was used for simply supported beams with knife edged ends which allowed rotation to take place. This arrangement was expected to be better as less friction would exist in the end joint than in a pin joint.

3.2.4 ADDITIONAL MASSES

The additional masses were made from steel slabs, which can be bolted onto the sliding mass by means of built-in bolts. Each of the masses weighed 5.8Kg and 0.975Kg and may satisfy different requirement during the vibration testing.

3.2.4 SIGNAL GENERATOR

A signal generator (Advanced Components Led., Hainault Essex England, L.F. Signal Generator, Type J, Model 2), was used to excite the shaker. The variable frequencies generated by the signal generator(D.C. excitor) to vibrate at different frequencies.

3.3.5 D.C. EXCITOR

The D.C. excitor (Advance Components Led., Hainault Essex England, Type V1) was used to excite the test beam. It was located above the beam by means of a vertical stand.

The stand could be adjusted to change the vertical location of the shaker so that the vibrating pin would be just touching the beam. The vibrating pin was held perpendicular to the top surface of the beam. This ensured an in-plane vibration of the beam and no bending moment in the vibrating pin.

3.3.6 ACCELEROMETER

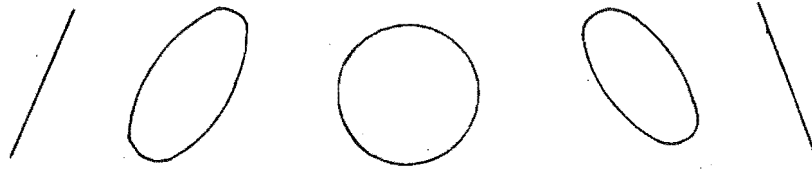
An accelerometer (Brüel & Kjær, Denmark, Type 4344, Serial no 376788, Range 5 Hz - 124 KHz), which was fixed onto the beam by means of plasticine, was connected to the oscilloscope. The accelerometer sensed the magnitude of vibration of the beam and relayed the signal to the oscilloscope.

3.3.7 OSCILLOSCOPE

The signal generator and the accelerometer were connected to the oscilloscope (Avalgamated Wireless NZ Ltd., Telequipment Oscilloscope DM 64). The two signals were received, The combined effects of these signals would be used to measure natural frequency and give what is called a lissajous figure.

In this experimental work, Lissajous figure was used to measure the natural frequency. The graphic

representation was shown below.



(1) (2) (3) (4) (5)

- (1) The frequency was low than the natural frequency.
- (2) It was approaching the natural frequency.
- (3) The exciting frequency was at the natural frequency.
- (4) The frequency was moving away from the natural frequency.
- (5) The frequency was higher than the natural frequency.

3.3.8 FREQUENCY COUNTER

The frequency counter (Hewlett Packard, model 5236B TIMER - COUNTER - DVM) gives accurate frequency reading of the beam vibration. The accelerometer picked up the vibrating signal of the beam and relayed it to the frequency counter .

3.3.9 TEST BEAMS

Eight uniform aluminium test beams with knife edged ends and varying initial curvature and eight other slightly curved uniform beams with holes for pin at the ends were used for experimental work. The deflections of the beams in the midspan were measured as explained below:

1. The profile of the beam was traced on a paper.
2. The ends of the tracing of the beams were connected to form the centre line of the undeflected beam.
3. The distance between the centre line of the traced profile and the straight line (undeflected centre line) was measured.

In some cases the shape of the beam while on the rig was traced and compared with the tracing of the same beam on the table. For simply supported beams there was not any significant difference. Some discrepancies were observed for clamped beam. However it was thought that this was not necessarily more accurate and the results from the tracing while the beam was outside the rig were used.

The dimension of the test beams was measured by micrometer and given in tabular form as shown below:

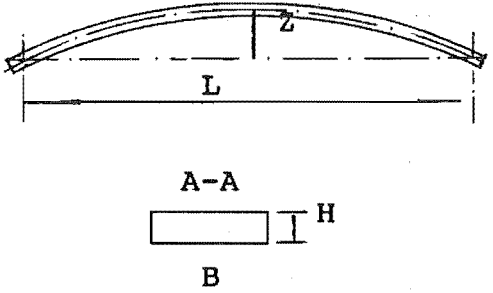
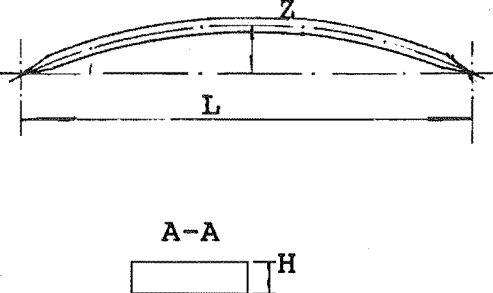
Test Beam	No	L	B	H	Qua	Z
	1	600	12.56	6.3	1	2.45
	2	600	12.56	6.3	1	7
	3	600	12.56	6.3	1	10.9
	4	600	12.56	6.3	1	22
	5	600	9.4	3	1	3.1
	6	600	9.4	3	1	5.5
	7	600	9.4	3	1	10.1
	8	600	9.4	3	1	19
	9	600	12.56	6.3	1	2.46
	10	600	12.56	6.3	1	7.1
	11	600	12.56	6.3	1	10.8
	12	600	12.56	6.3	1	22.1
	13	600	9.4	3	1	3
	14	600	9.4	3	1	5.4
	15	600	9.4	3	1	10
	16	600	9.4	3	1	19.1

Figure (3.4) Drawing of test beams(mm)

In testing of the pinned beams , the beams was held in place by inserting a pin through the drilled hole in the trunnion of the end mass and the drilled hole in the beam at each end. The pin joint ensured that the test beam could be removed easily and quickly, this also ensured in-plane vibration of the beam and no bending moment of the beams

was transmitted to the sliding end masses.

In the testing of simply supported beams with knife edged ends, the beams were held in place by adjusting the "adjusting screw" to ensure, that while a small axial force may be induced in the beam there would be no gap between the V-grooves and the knife edges of the beam.

In the testing of the clamped beams with initial curvature and sliding end mass, the beams were clamped by tightening the screw in the clamp block which ensured in-plane vibration of the beam and the bending moment at the ends of the beams were fully transmitted to the sliding end masses.

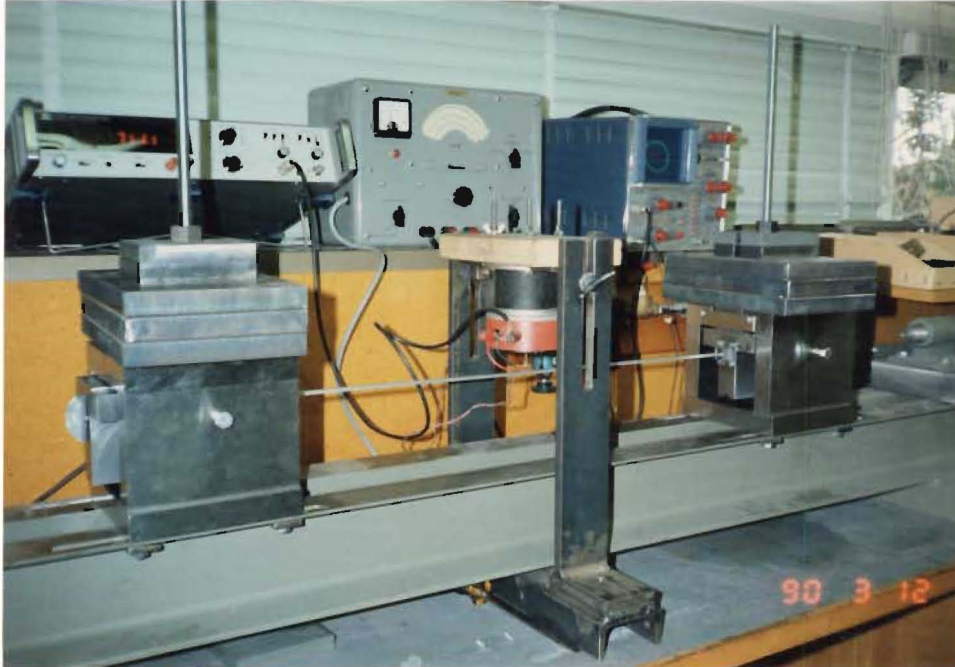
Once the test beam was set, the excitor was positioned on top of it . The vertical stand provided an adjustable platform for the height of the excitor with respect to the test beam. The height of the excitor was adjusted so that its vibrating pin was just touching the beam. The pin was not allowed to exert any significant load onto the curved beam as this might affect the experimental results. Then, all the electrical equipments were switched on. The excitor would then excite the beam. The vibration that the beam underwent was picked up by the accelerometer, which was connected to the oscilloscope. Meanwhile, the out put signal from the beam was also transmitted to the frequency counter via the oscilloscope. The signal from the generator was varied so that the resulting vibrating signal reached its first maximum amplitude ie, the fundamental natural

output in the oscilloscope screen. Generally, it could also be read by acoustic means as the beam vibrating at resonant frequency had high sound energy. The frequency reading was then recorded from the frequency counter which showed the output frequency from the beam. The first mode natural frequency was confirmed by moving the accelerometer along the beam while observing the signal output from the oscilloscope. The absence of any phase shift indicated that the beam was vibrating in its fundamental mode.

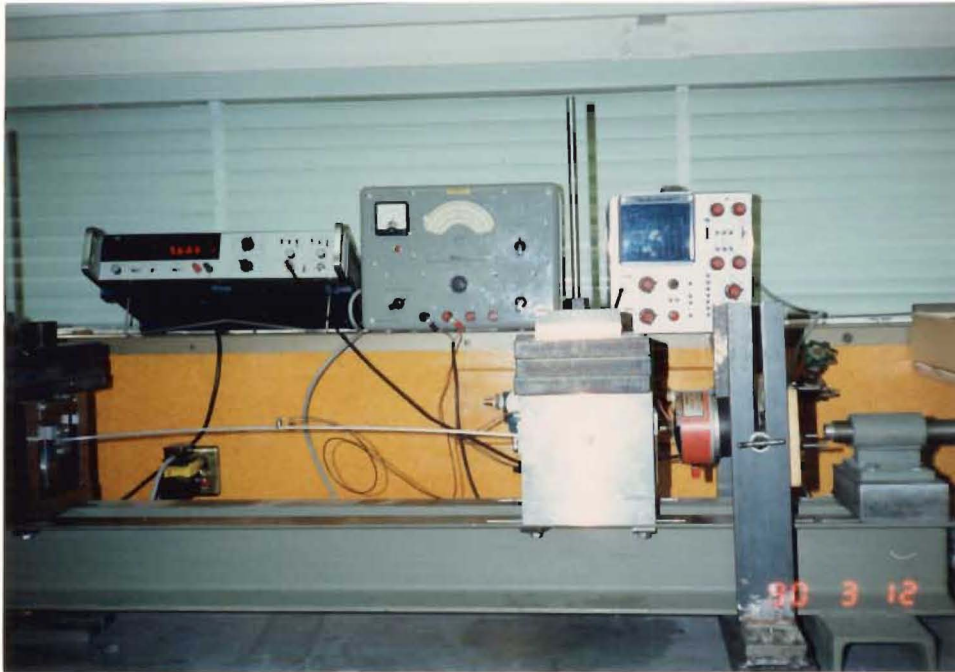
For each beam tested, twelve additional weights that included 4 weights, each of which weighed 0.975Kg and 8 weights, each of which weighed 5.8KG were added progressively to the original end mass of 0.9Kg. Weights were added onto the end masses by bolting them onto the built-in bolt in the sliding mass as shown in figure(3.2). This provided a very easy, fast and reliable method of adding or removing weight from the end blocks.

According to the theoretical analysis, it was expected that there would be two natural frequencies having fundamental transverse mode. However, when the experimental work was carried out, it was found that the higher fundamental frequency was hard to be detected. This problem was solved by changing the direction of excitation from transverse to longitudinal (Photograph 3.2). Through this way, clear Lissajous figures were observed and modes were checked by way of moving accelerometer along the length of the beam, which showed there was not a phase shift and indicated that the

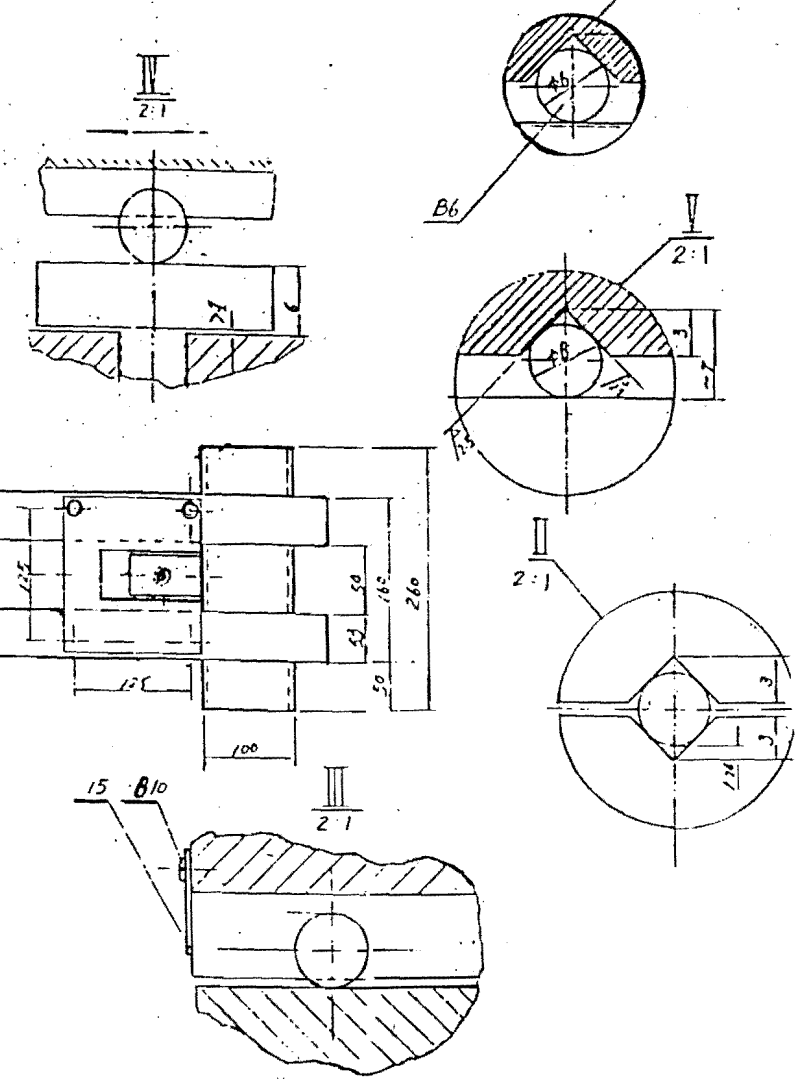
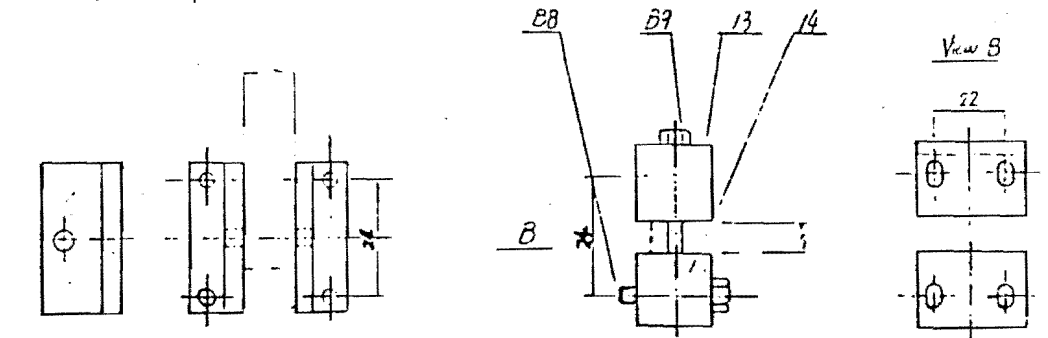
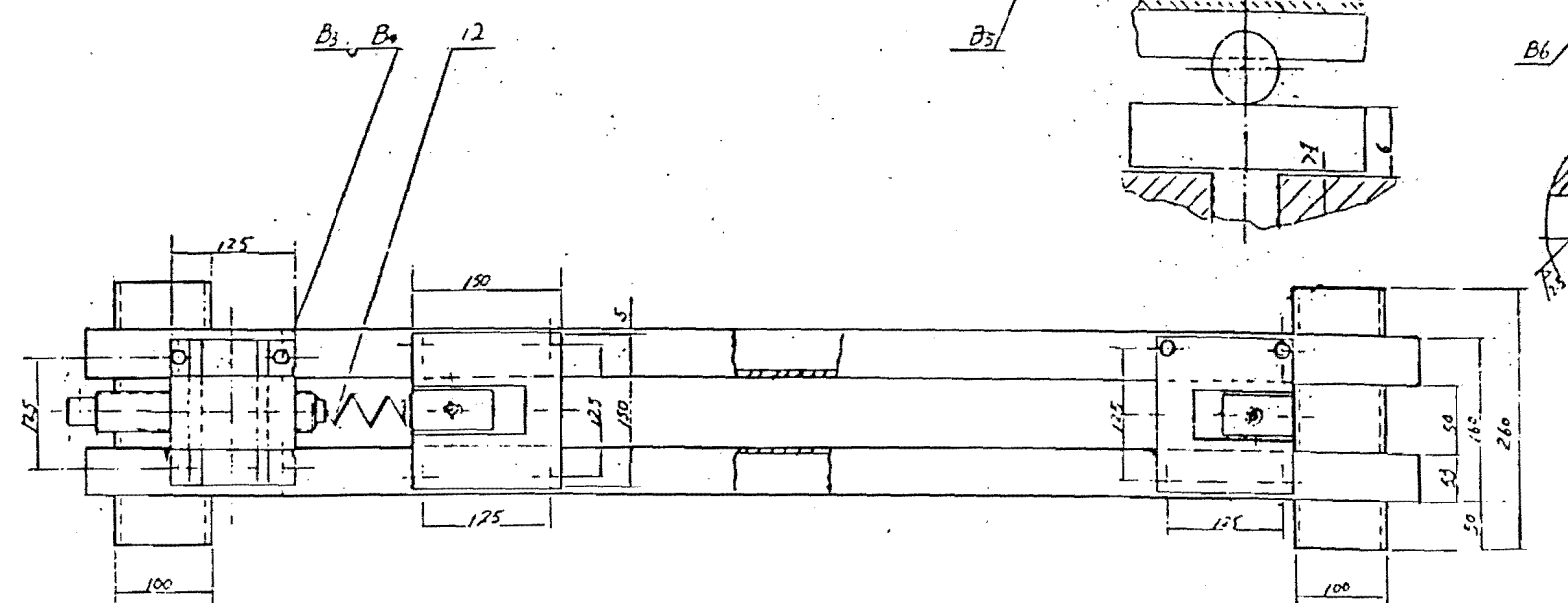
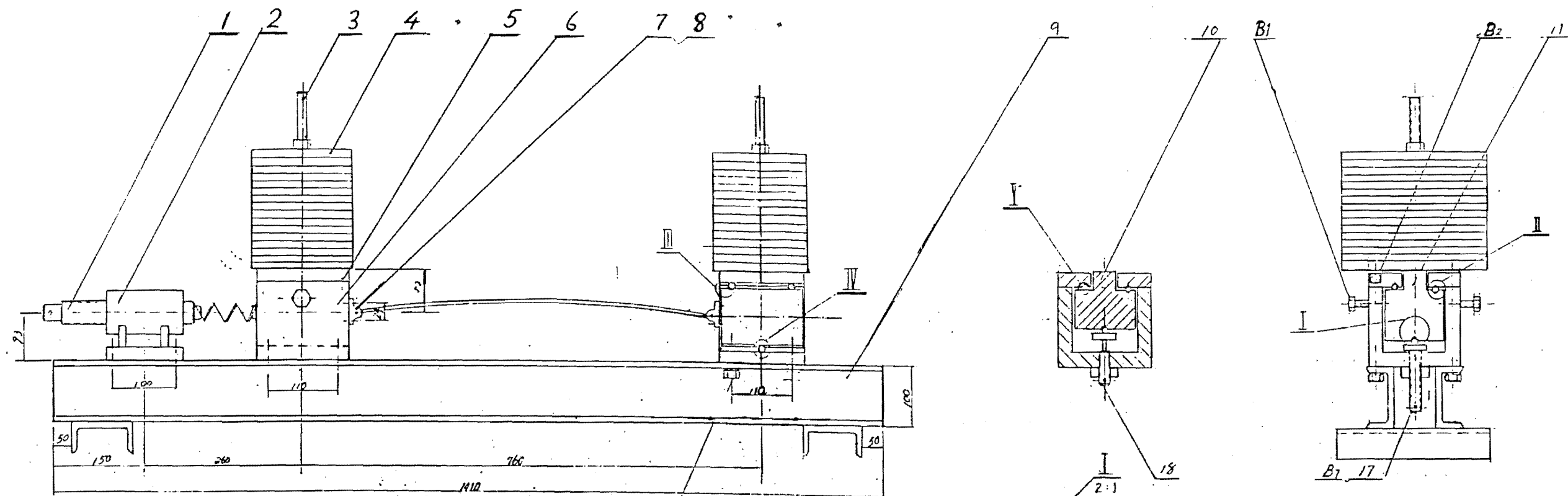
the beam was vibrating in its fundamental mode.



Photograph(3.1) A setup of testing apparatus



Photograph(3.2) Excitor is set up in longitudinal direction



B10	M4x20 screw	8			
B9	4x35 screw	1			
B8	4x40 screw	4			
B7	6 nut	3			
B6	6 ball	8			
B5	6x30 screw	6			
B4	8 nut	4			
B3	8x40 screw	4			
B2	8x30 screw	8			
B1	8x60 screw	4			
15	block plate	4	A3	.3x4	
14	fixed support II	1	45		
13	fixed support I	1	45		
12	spring	1			
11	sliding block II	2	45	.8x2	
10	sliding block I	1	45	.8	
9	shassis	1	4		may be modified
8	simple supportII	2	A3	.5x2	
7	simple support I	2	A3	.2x2	
6	fixed base	2	A	10.2	
5	lid	2	4	3.6x2	
4	weight block	16	A	5x16	
3	M12x380	2	A3	3x2	
2	shaft base	1		4.12	may be modified
1	shaft thread	1	45	2.12	may be modified
Item	Description	No.	mate.	Kg	

17	Adjusting Screw II	2	45	0.0782	
16	Adjusting Screw I	2	45	0.0542	

Test Equipment			name	Yueming
			scale	1:5

Figure(3.1) Test equipment

CHAPTER 4 RESULTS & DISCUSSION

4.1 THEORETICAL RESULTS OF SIMPLY SUPPORTED BEAMS

In chapter 2, expressions for the natural frequencies of curved simply supported beams corresponding to the fundamental transverse mode were given in equations (2,2,10) and (2,4,25). These equations were solved by using a computer program. As the equation for Ω is quadratic there are two values of fundamental frequencies for a given value of end mass. Theoretical results show that there are two different natural frequencies corresponding to the same fundamental transverse mode. Table(4.1.1) - table(4.1.4) are theoretical results corresponding to equations (2.2.10) and (2.4.25) as shown below.

Beam 12.56x6.3x600 mm

MASS Kg	Z=2.45		Z=7		Z=10.9		Z=22	
	Ω_1	Ω_2	Ω_1	Ω_2	Ω_1	Ω_2	Ω_1	Ω_2
1.0	43.2	709	40.9	717	36.3	748	28.3	791
2.0	43.0	502	40.4	513	35.8	542	27.6	613
3.0	42.9	410	39.9	424	35.6	458	26.9	540
4.0	42.8	356	39.3	371	35.4	405	26.5	500
5.8	42.7	319	38.8	336	34.8	367	26.3	466
6.8	42.6	298	38.5	314	34.7	341	26.0	446
7.8	42.3	276	38.0	293	34.6	322	25	436
8.8	42.2	259	37.6	277	33.9	307	23.9	427
9.8	42.1	244	37.2	263	33.1	296	23.0	420
10.8	42.0	227	36.4	243	31.7	278	21.3	414
15.8	41.5	187	34.6	211	29.2	251	18.4	396
20.8	40.9	164	33.1	192	27.1	235	16.5	387
25.8	40.4	149	31.7	180	25.4	225	15	381
30.8	39.8	138	30.5	172	24	218	13.9	377
35.8	39.3	130	29.4	166	22.7	213	13	374
40.8	38.8	123	28.4	160	21.7	209	12.2	372
45.8	38.3	118	27.5	156	20.8	206	11.6	370
50.8	37.9	107	26.7	153	20.4	204	11.0	368
70.8	36.6	94	24.6	144	17.0	198	9.4	365
80.8	35.9	90	22.9	141	16.1	197	8.9	363
500	21.1	61	10.5	123	7.1	182	3.6	356

Table(4.1.1) Theoretical results of curved simply supported Beams(12.56x6.3x600mm) with sliding end masses, which neglect axial inertia of the beam.

Beam 9.4x3x600 mm

MASS Kg	Z=3.1		Z=5.5		Z=10.1		Z=19	
	Ω_1	Ω_2	Ω_1	Ω_2	Ω_1	Ω_2	Ω_1	Ω_2
1.0	19.3	425	18.7	435	16.8	474	11.7	521
2.0	19.2	303	18.4	325	16.2	369	11.2	427
3.0	19.1	249	18.1	265	15.6	328	10.7	390
4.0	18.9	217	17.7	216	15.0	288	10.2	371
5.8	18.8	200	17.5	212	14.4	254	9.7	365
6.8	18.7	182	17.4	196	13.8	239	9.2	352
7.8	18.6	169	17.2	184	13.3	229	8.7	345
8.8	18.5	159	16.9	175	12.9	222	8.3	340
9.8	18.4	151	16.6	167	12.5	216	7.9	337
10.8	18.2	137	16.1	156	12.1	207	7.6	331
15.8	17.7	117	15.0	138	10.7	194	6.4	323
20.8	17.2	105	14.1	128	9.7	187	5.7	319
25.8	16.7	97	13.3	122	8.9	183	5.1	316
30.8	16.3	91	12.7	117	8.3	179	4.7	314
35.8	15.9	87	12.1	114	7.8	177	4.2	313
40.8	15.4	83	11.6	111	7.3	176	4.1	312
45.8	15.1	80	11.2	109	7.0	174	3.9	311
50.8	14.8	78	10.8	107	6.7	173	3.7	311
70.8	13.6	72	9.6	103	5.8	170	3.2	309
80.8	13.2	69	9.1	101	5.4	169	3.0	309
500	6.5	56	4.0	92	2.2	164	1.2	306

Table (4.1.2) Theoretical results of curved simply supported beams(9.4x3x600mm) with sliding end masses, which neglect axial inertia of the beam.

Beam 12.56x6.3x600 mm

MASS Kg	Z=2.45		Z=7		Z=10.9		Z=22	
	Ω_1	Ω_2	Ω_1	Ω_2	Ω_1	Ω_2	Ω_1	Ω_2
1.0	44.2	686	43.0	698	37.5	720	30.3	769
2.0	44.0	482	42.5	495	36.9	513	29.5	588
3.0	43.9	392	40.8	408	36.7	430	28.7	525
4.0	43.7	341	40.1	356	36.5	385	28.2	488
5.8	43.6	307	39.3	328	35.7	355	27.8	460
10.8	42.6	221	36.8	245	32.5	280	21.6	415
15.8	42.1	182	35.0	211	29.8	251	18.7	396
20.8	41.5	159	33.4	192	27.5	235	16.7	387
25.8	40.9	144	32.1	180	25.7	225	15.2	381
30.8	40.3	133	30.9	172	24.2	218	14.0	377
35.8	39.8	124	29.7	166	22.8	213	13.1	374
40.8	39.2	116	28.6	160	21.8	209	12.2	372
45.8	38.5	112	27.5	156	20.8	206	11.6	370

Table(4.1.3) Theoretical results of curved simply supported beams with sliding end masses, which include axial inertia of the beam.

Beam 9.4x3x600 mm

MASS Kg	Z=3.1		Z=5.5		Z=10.1		Z=19	
	Ω_1	Ω_2	Ω_1	Ω_2	Ω_1	Ω_2	Ω_1	Ω_2
1.0	19.9	401	19.1	415	17.6	452	12.4	499
2.0	19.6	283	18.8	307	16.8	352	11.9	408
3.0	19.3	231	18.4	247	15.9	325	11.3	376
4.0	18.9	204	18.0	211	15.4	278	10.7	360
5.8	18.8	189	17.2	208	15.0	248	10.3	358
10.8	17.8	142	15.8	161	12.8	212	7.8	332
15.8	17.0	118	15.0	141	11.0	196	6.6	325
20.8	16.8	107	14.7	130	9.9	188	5.7	319
25.8	16.4	98	13.5	123	9.0	183	5.2	316
30.8	16.0	80	13.0	117	8.3	179	4.8	314
35.8	15.8	75	12.4	114	7.8	177	4.4	313
40.8	15.6	72	11.7	111	7.3	176	4.2	312
45.8	15.3	70	11.2	98	7.0	174	3.9	312

Table(4.1.4) Theoretical results of curved simply supported beams with sliding end masses, which include axial inertia of the beam.

Comparing tables (4.1.1) & (4.1.3), with the tables (4.1.2) and (4.1.4) the disagreement between two equations can be seen to increase with the value of initial curvature; the disagreement is more pronounced for the second fundamental mode. The frequency value which considers axial inertial force of the beam is lower than that neglecting one. for first fundamental mode. For the second fundamental mode, the results is contrary to the first fundamental mode. Further discussion will be given in section 4.2.

4.2 DISCUSSION AND COMPARISON OF EXPERIMENTAL AND THEORETICAL RESULTS OF CURVED SIMPLY SUPPORTED BEAMS WITH SLIDING END MASSES

The experimental and theoretical results of test beams from No1 to No16 Fig(3.4) are compared graphically in Figures(4.2.1 - 4.2.8). In the case the of first fundamental natural frequency, the agreement between the theoretical and experimental results is reasonable. The measured natural frequencies of knife edged beams are slightly lower than the corresponding values for the pin ended beams. The agreement between the theoretical and experimental results for knife edged beams are marginally better than that for pin ended beams. This may be due to that the friction existing in the ends of the simply supported beam may induce bending moment in the end of the beam, change the assumptive boundary-condition of simply supported beam, and influence the natural frequency of the beam. As the end mass tends to infinity, the value of first fundamental frequency tends to zero. This may be taken as that the ratios of longitudinal motion to the transverse motion tends to increase.

For the curves of second fundamental frequency, the theoretical natural frequency obtained by including the effect of axial inertial force of the beam are slightly lower than that calculated by neglecting the axial inertial force of the beam for the end masses in the range of 0-20Kg. However, the reverse is exhibited for the curves corresponding to

the first fundamental mode.

The agreement between the theoretical and experimental results is slightly improved by including the effect of axial inertia in the theoretical analysis. It is interesting to note that the discrepancy between the two theoretical results almost disappear for the end masses above 20 Kg. This indicates that the effect of axial inertia decreases with increasing end masses.

Comparing the two fundamental modes, it was found that the frequency of the second fundamental mode tends to a fixed value when the end mass tends to infinity whereas for the same condition the first one approaches zero. This shows that the first mode is predominantly longitudinal and the second one is transverse as end masses become very large.

From figures(4.2.1-4.2.10), the following observations regarding the influence of the beam dimension and shape on the natural frequencies may be made:

(1) Frequencies of the beam increase with the radius of gyration of the beam.

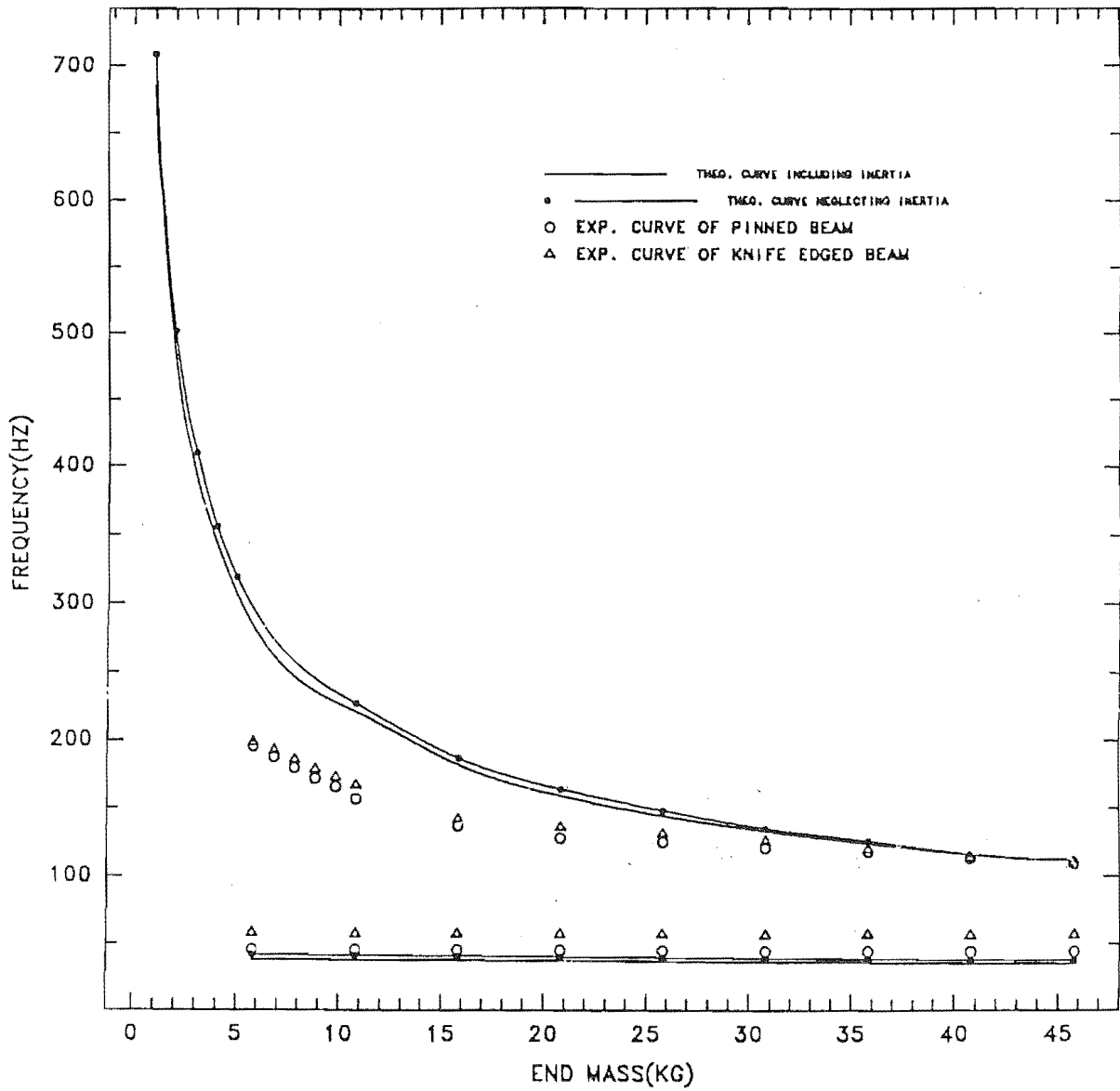
(2) For first fundamental mode, the frequency decreases when the initial curvature Z is increased. However, the reverse is exhibited for second fundamental mode. This is illustrated in Figures(4.2.9) and (4.2.10).

(3) The difference between the values of first and

second fundamental natural frequencies tend to increase when the initial curvature z increases. For the 12.56x6.3x600mm beams with end mass ($M=20\text{Kg}$), the ratio of two frequencies increase from 1:6.5 to 1:10 when the initial curvature z increases from 2.45 to 22 mm. For the 9.4x3x600mm beams with the end mass ($M=20\text{Kg}$), the ratio of them increases from 1:9 to 1:30 when the initial curvature z increase from 3.1 to 19 mm as shown in figures(4.2.1) - (4.2.8).

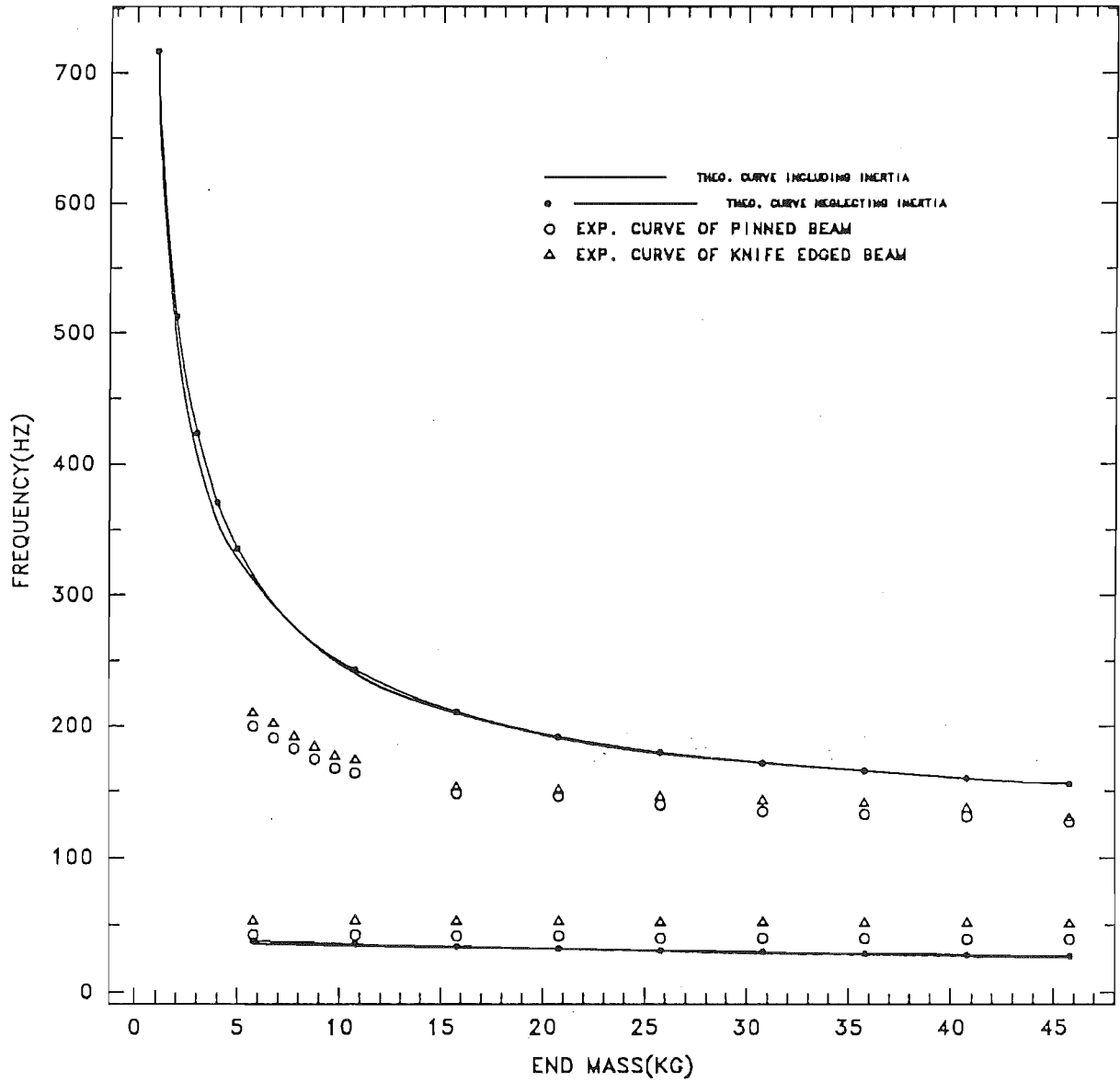
(4) For the second fundamental natural frequencies, the variation of the square of (Ω_t/Ω_0) with the square of (Z/r) is linear. However it is not possible to verify this experimentally (see figures(4.2.9) and (4.2.10)) as there are only 4 points and in general they do not form straight lines.

BEAM(12.56*6.3*600mm) Z=2.45



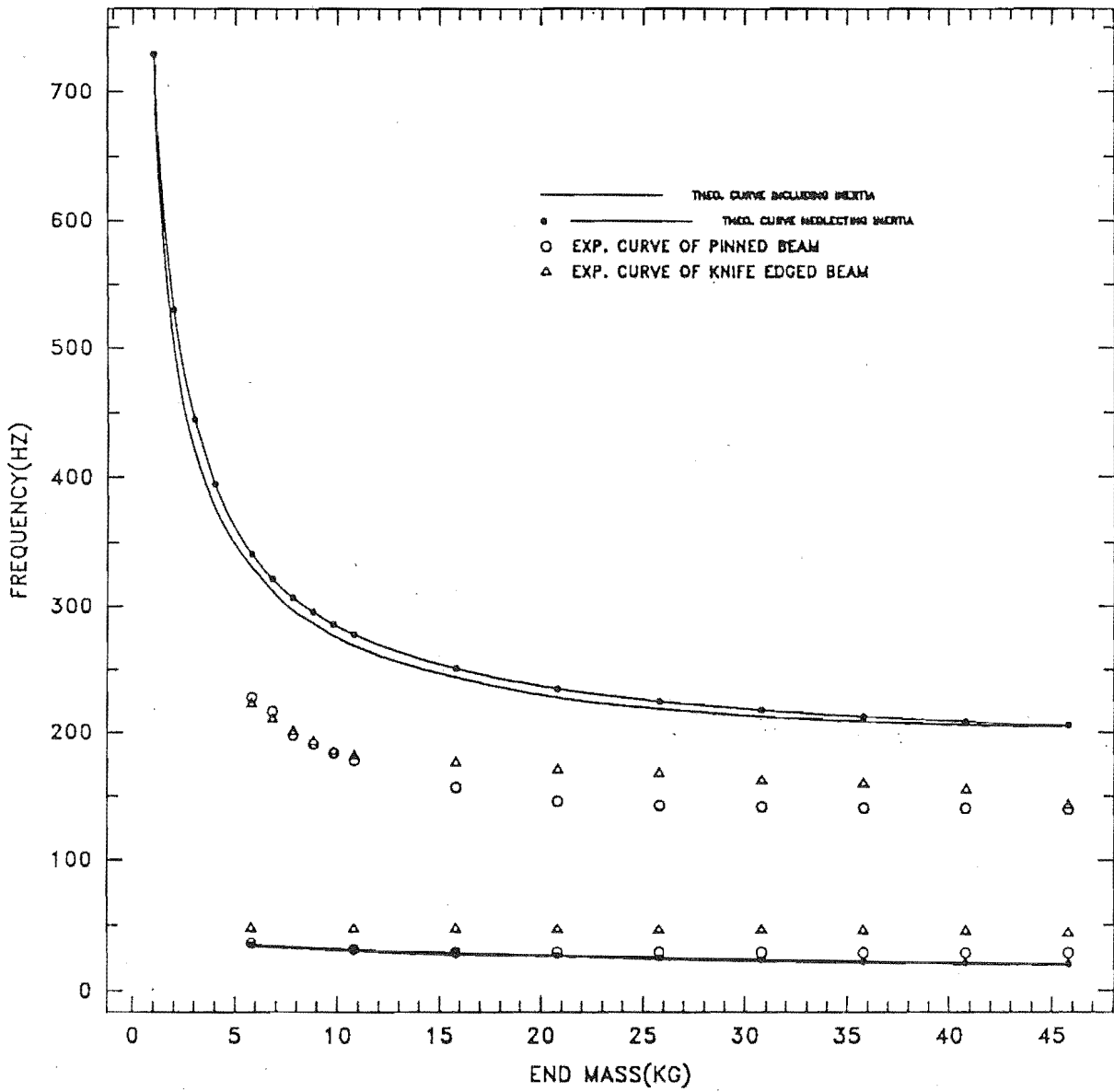
Figure(4.2.1) Frequency(Hz) of simply supported beam vs. end mass(Kg)

BEAM(12.56*6.3*600mm) Z=7.00



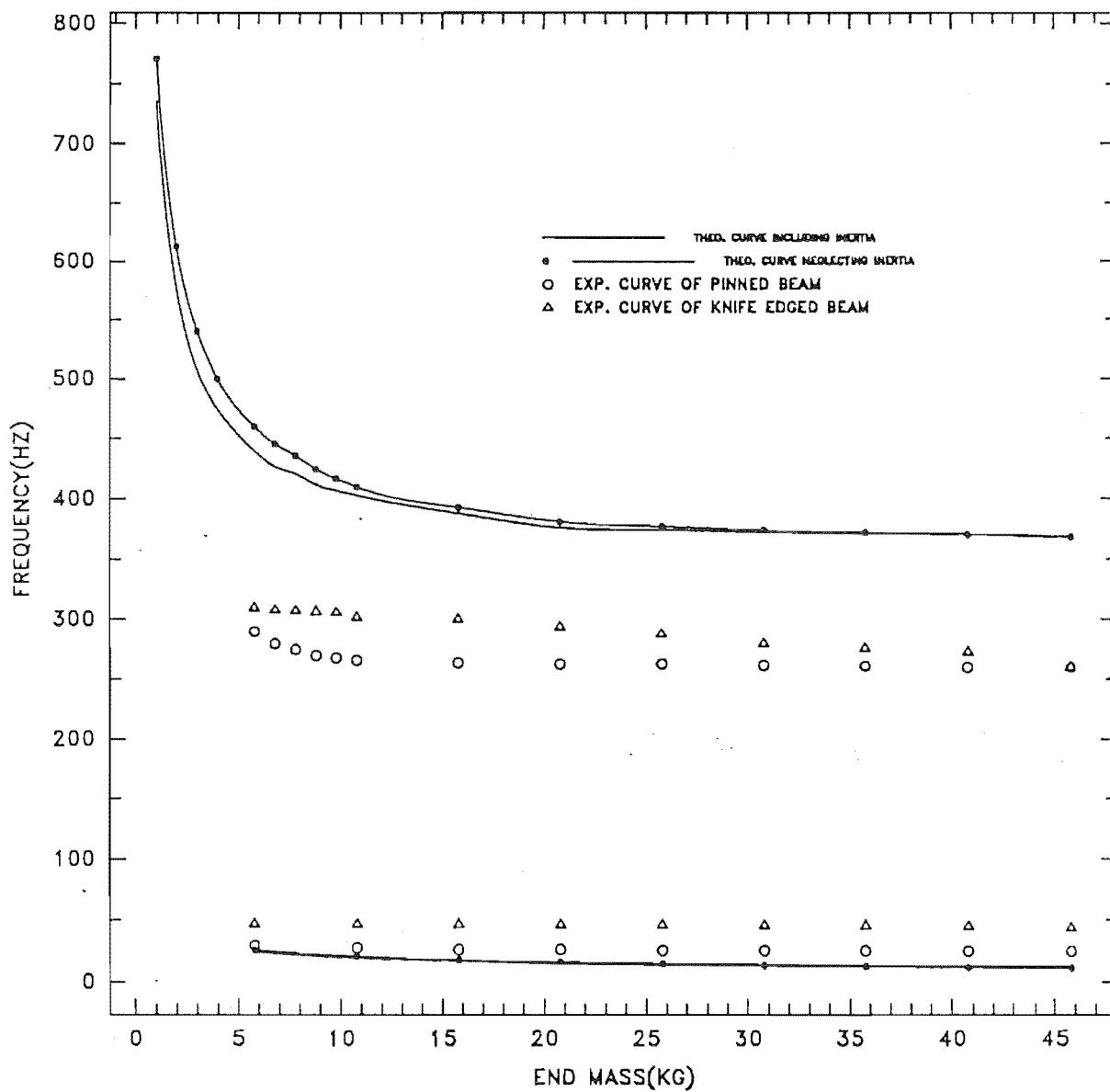
Figure(4.2.2) Frequency(Hz) of simply supported beam vs. end mass(Kg)

BEAM(12.56*6.3*600mm) Z=10.90



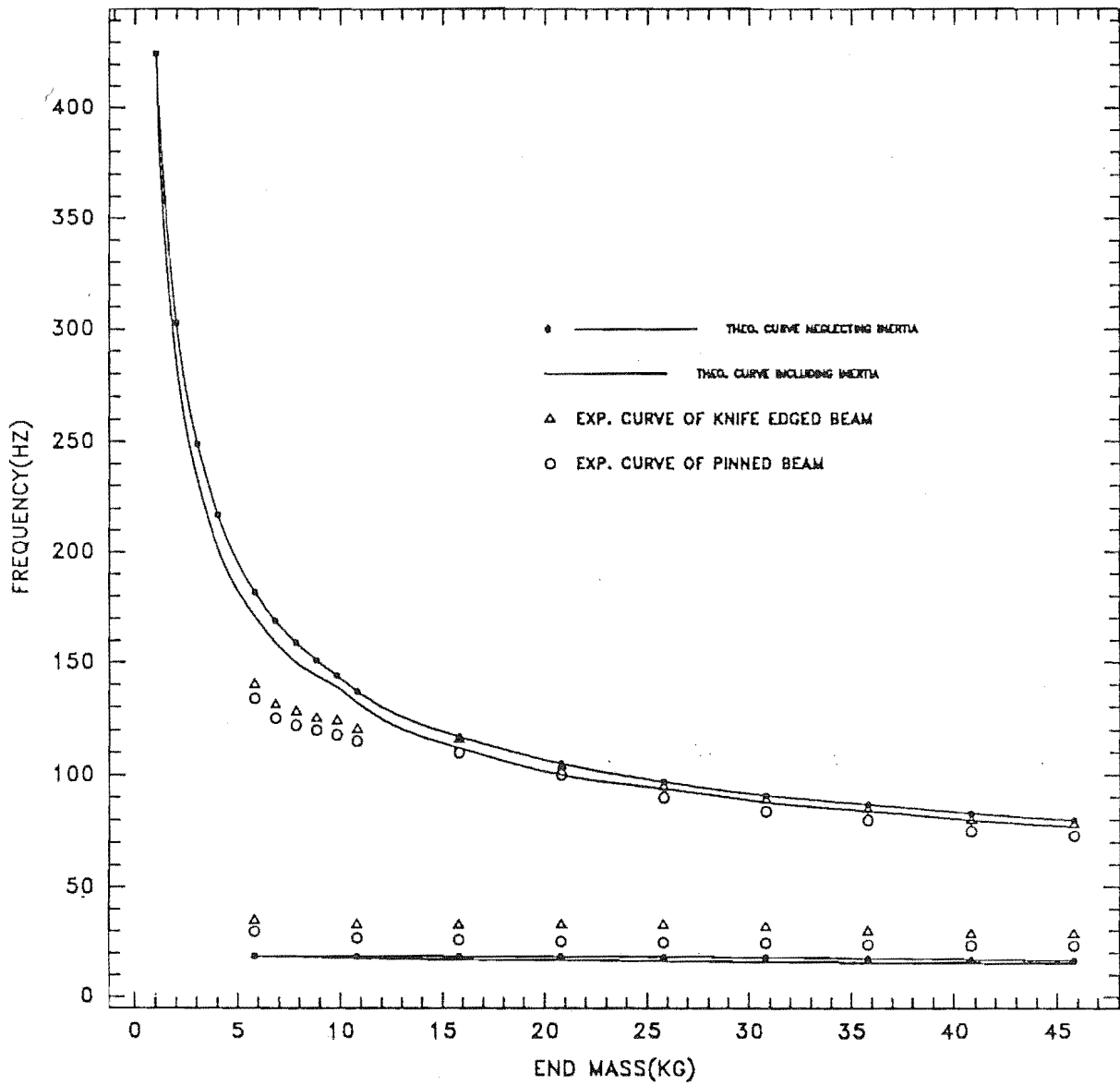
Figure(4.2.3) Frequency(Hz) of simply supported beam vs. end mass(Kg)

BEAM(12.56*6.3*600mm) Z=22.00



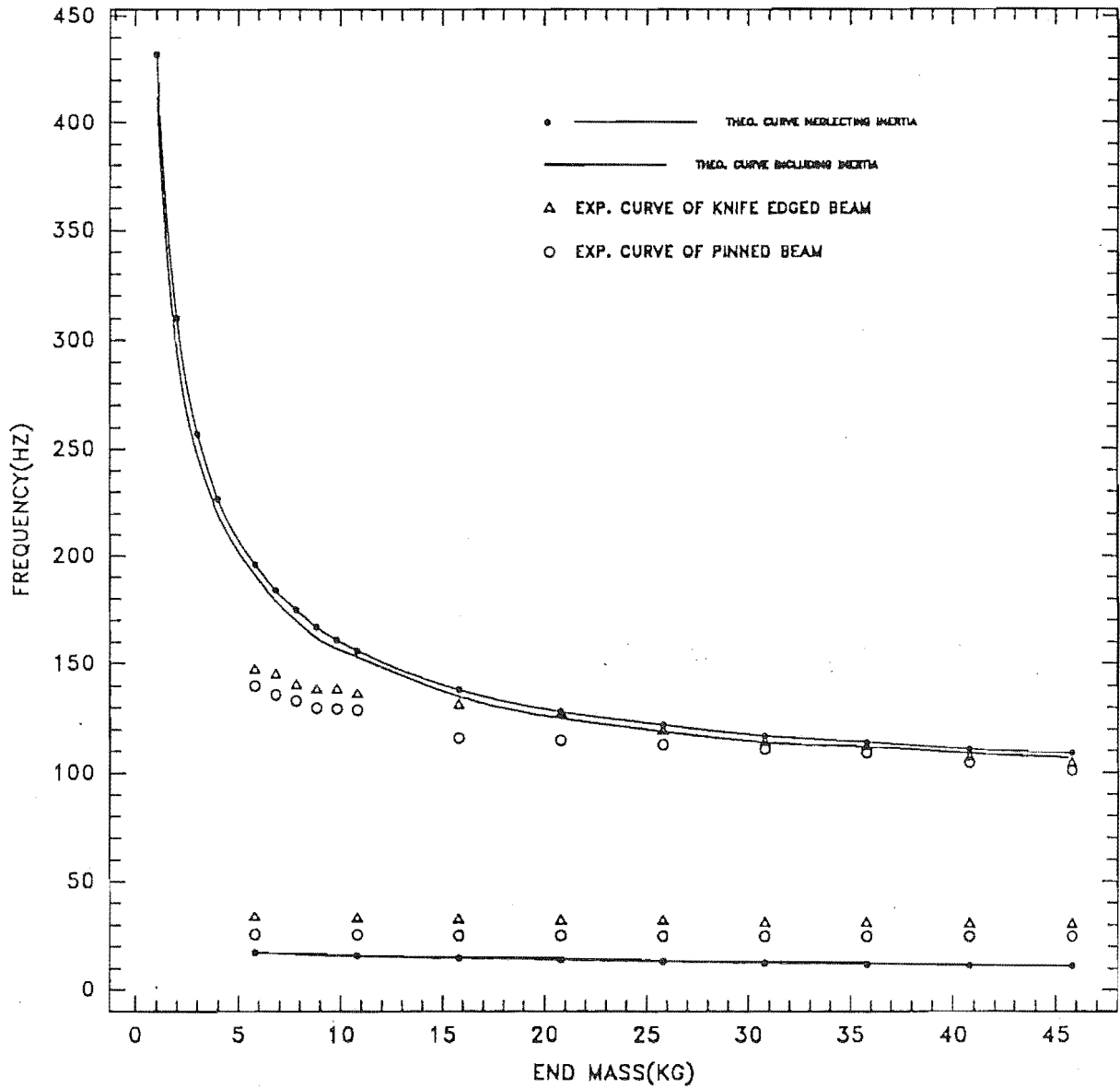
Figure(4.2.4) Frequency(Hz) of simply supported beam vs. end mass(Kg)

BEAM(9.4*3.0*600mm) Z=3.1



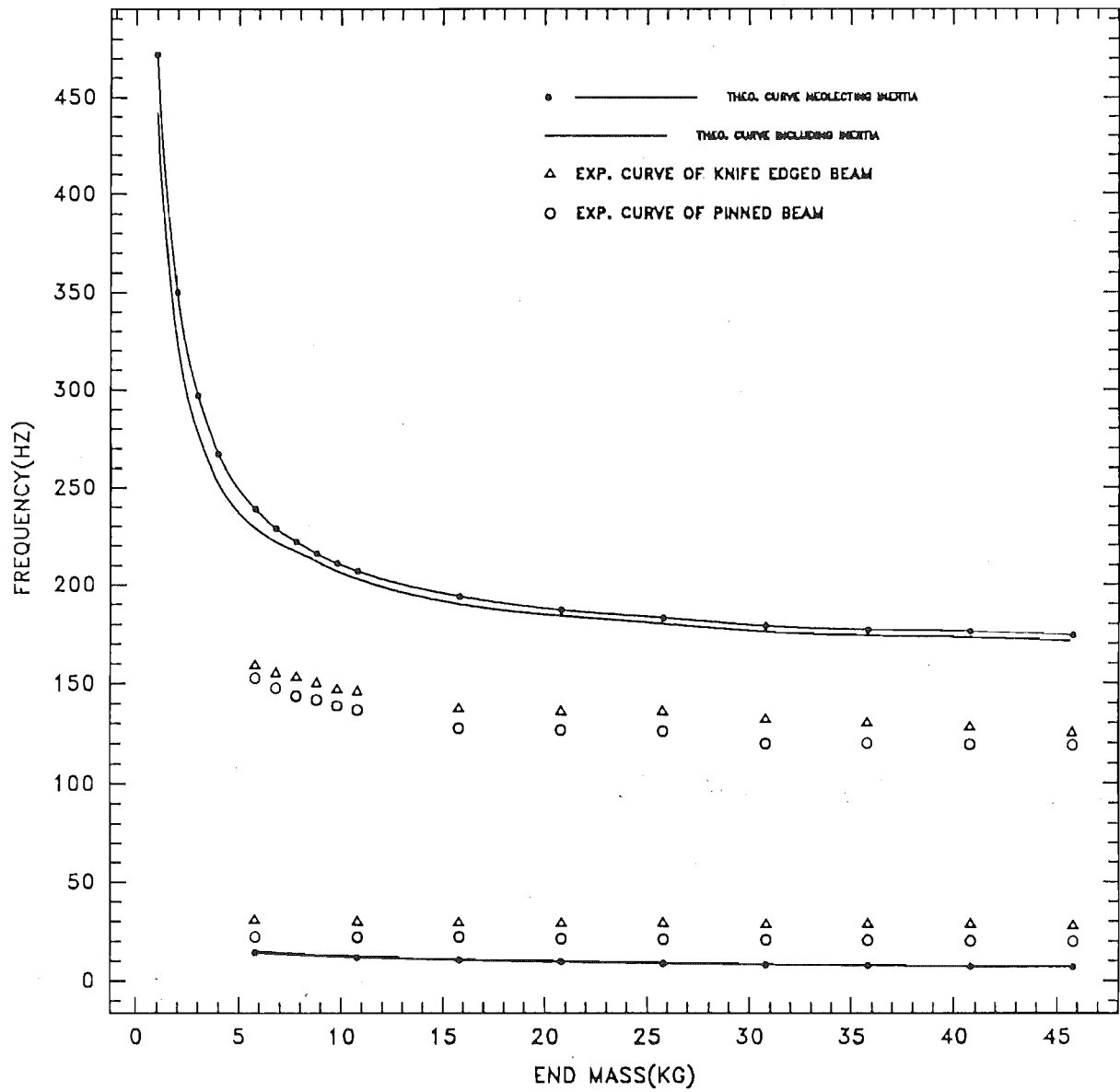
Figure(4.2.5) Frequency(Hz) of simply supported beam vs. end mass(Kg)

BEAM(9.4*3.0*600mm) Z=5.5



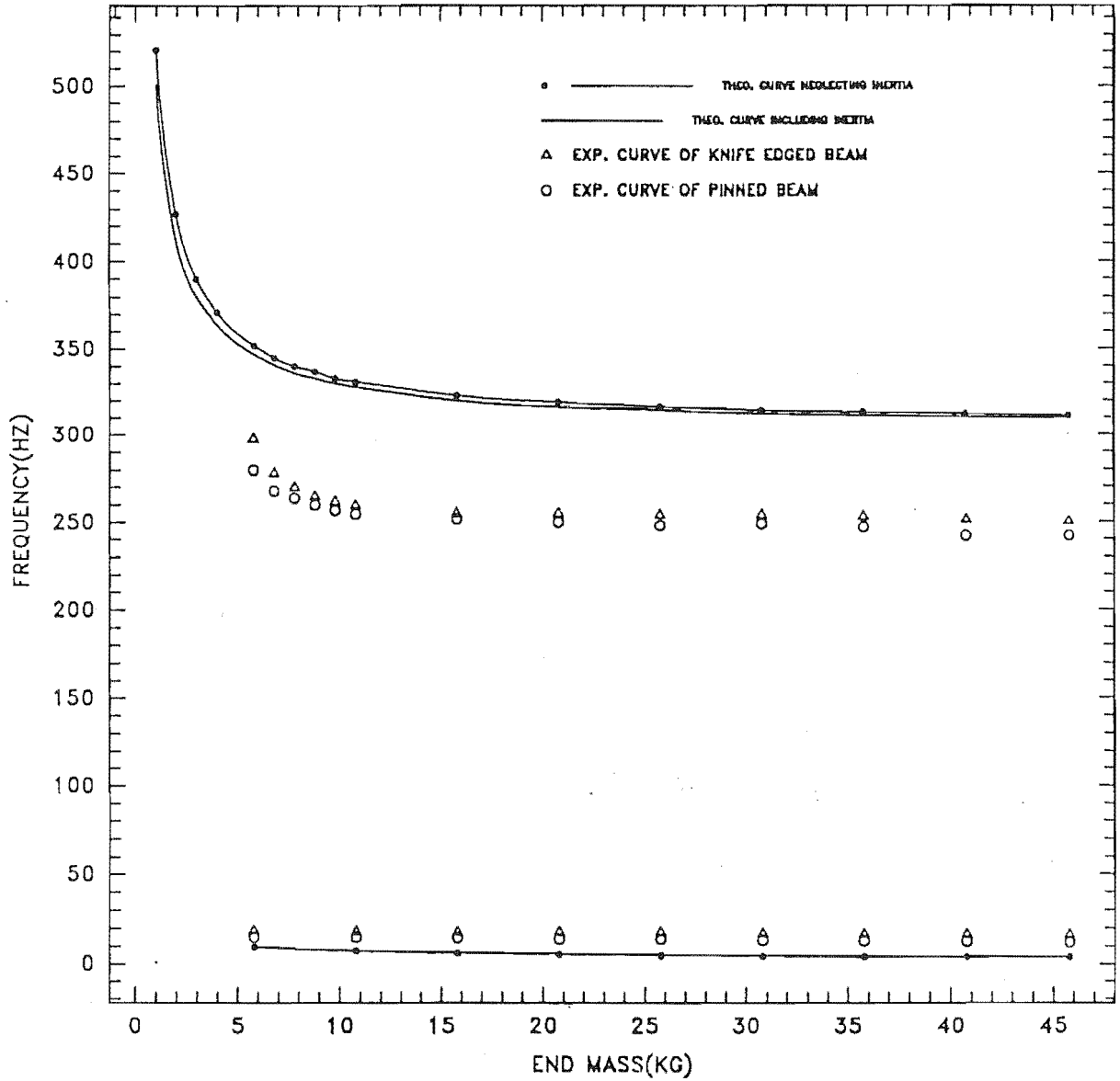
Figure(4.2.6) Frequency(Hz) of simply supported beam vs. end mass(Kg)

BEAM(9.4*3.0*600mm) Z=10.10

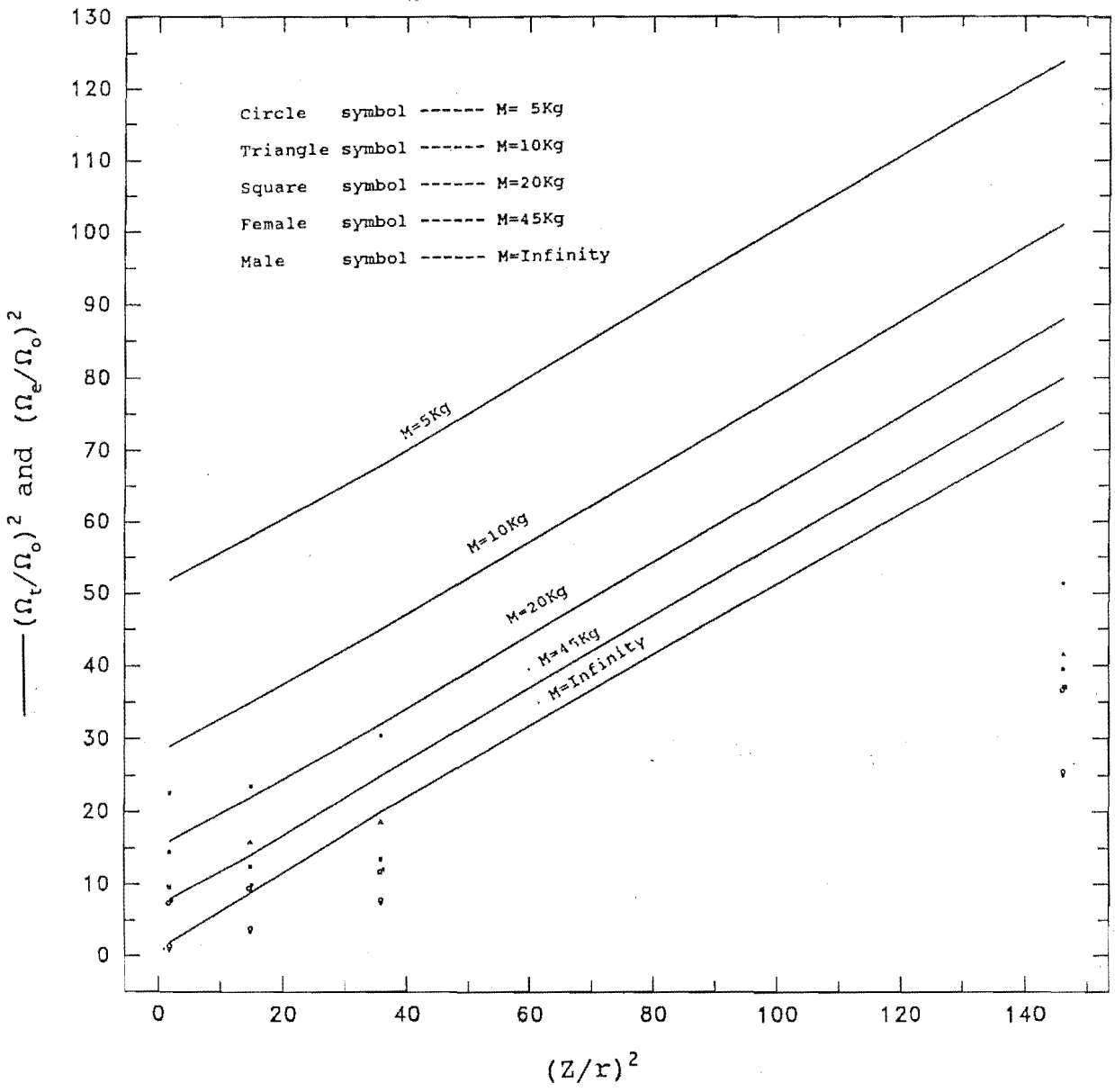


Figure(4.2.7) Frequency(Hz) of simply supported beam vs. end mass(Kg)

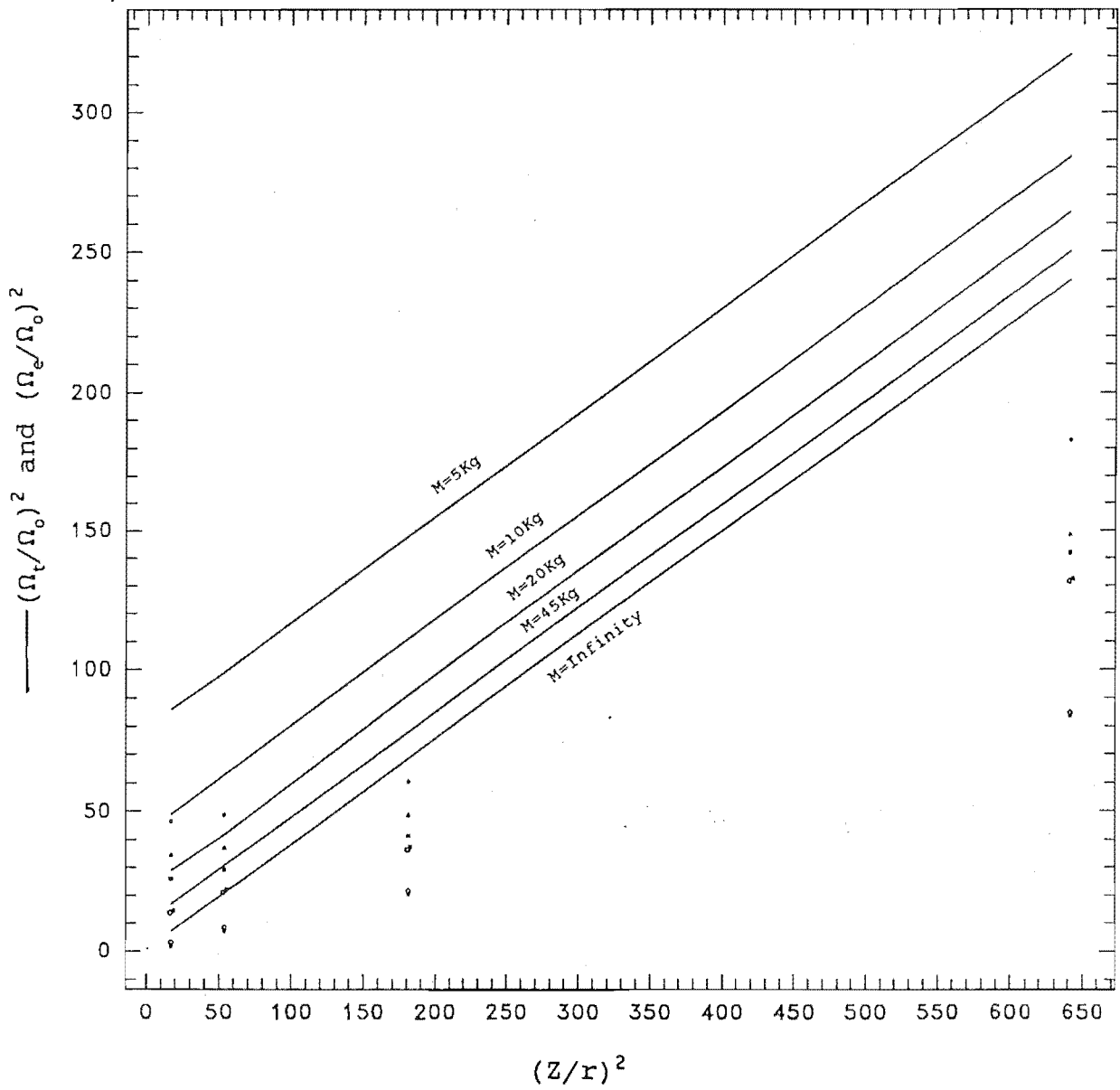
BEAM(9.4*3.0*600mm) Z=19.00



Figure(4.2.8) Frequency(Hz) of simply supported beam vs. end mass(Kg)



Figure(4.2.9) $(\Omega_t/\Omega_0)^2$
 and $(\Omega_e/\Omega_0)^2$ vs. $(Z/r)^2$
 of simply support beams (12.56
 x6.3x600mm beam)



Figure(4.2.10) $(\Omega_t/\Omega_0)^2$ and $(\Omega_e/\Omega_0)^2$ vs. $(Z/r)^2$ of simply supported beams (9.4x3x600mm beam)

Although the agreement between the theoretical and experimental result of simply supported slightly curved beams is good, some discrepancy still exists particularly for small masses. This may be attributed at least partly to the following factors:

(1) Presence of some restraint against rotation of the beam at the edges.

(2) Friction at the ball bearings against the free motion of sliding end mass in axial direction.

(3) Shape of the initial curvature of the beam being different from the assumed shape. Further investigation is given in appendix A.

(4) Presence of initial residual stresses since the beams were not stress relieved prior to testing.

(5) Measurement errors and errors due to simplifying assumptions made in modelling as explained in appendices A and C.

As expected, the above listed factors have not significantly influenced the results of natural frequencies of simply supported beam with small initial curvature except for small end masses and sliding end mass so reasonable results were obtained in this work.

4.3 THEORETICAL RESULTS OF CURVED CLAMPED BEAM WITH SLIDING END MASSES

In the chapter 2, the expressions of natural frequency of clamped beam was given in equation(2.3.9). As the equation for Ω is also quadratic, there are two values of fundamental frequencies for a given value of end mass.

It is interesting to note that like simply supported beam, there are two different natural frequencies corresponding to the fundamental transverse mode of a clamped beam. these results are shown in table(4.3.1) and table(4.3.2).

Beam 12.56x6.3x600 mm

MASS Kg	Z=2.45		Z=7		Z=10.9		Z=22	
	Ω_1	Ω_2	Ω_1	Ω_2	Ω_1	Ω_2	Ω_1	Ω_2
5.8	90.6	309	68.3	410	55.4	505	32.1	871
6.8	89.8	288	65.5	394	52.4	493	29.9	864
7.8	89.0	271	63.1	382	49.9	483	28.1	858
8.8	88.2	257	60.8	373	47.7	476	26.6	854
9.8	87.3	246	58.8	366	45.8	470	25.3	851
10.8	86.5	237	57.0	359	44.1	465	24.2	848
15.8	82	205	49.9	339	37.7	450	20.2	839
20.8	78	187	44.9	329	33.4	441	17.7	835
25.8	75.3	176	41.1	322	30.4	436	15.9	832
30.8	72	162	38.2	318	28.0	433	14.6	830
35.8	69.2	158	35.8	314	26.1	430	13.6	829
40.8	66.5	155	33.8	312	24.6	428	12.7	828
45.8	64.1	141	32.1	310	23.3	427	12.0	827
100	47.6	133	22.3	301	16.0	420	8.1	823
500	22.6	132	10.2	295	7.2	416	3.6	821
1000	16.1	90	7.2	294	5.1	415	2.6	821

Table(4.3.1) Natural frequencies of clamped beams with sliding masses and initial curvature

Beam 9.4x3x600 mm

MASS Kg	Z=3.1		Z=5.5		Z=10.1		Z=19	
	Ω_1	Ω_2	Ω_1	Ω_2	Ω_1	Ω_2	Ω_1	Ω_2
5.8	37.3	213	29.3	271	19	415	10.9	726
6.8	36.3	202	27.9	262	17.9	410	10.1	723
7.8	35.2	193	26.7	256	16.9	405	9.5	721
8.8	34.2	188	25.7	251	16.0	402	8.9	719
9.8	33.5	183	24.7	247	15.3	400	8.5	718
10.8	32.8	177	23.9	244	14.6	398	8.1	717
15.8	29.6	162	20.6	233	12.3	391	6.7	713
20.8	29.4	153	18.4	227	10.8	388	5.9	711
25.8	25.3	149	16.8	224	9.7	385	5.3	710
30.8	23.6	146	15.5	221	8.9	384	4.8	709
35.8	22.3	143	14.5	219	8.3	383	4.5	709
40.8	21.2	141	13.7	218	7.8	382	4.2	708
45.8	20.4	140	13.0	217	7.4	382	4.0	708
100	14.4	133	9	212	5.0	379	2.7	706
500	6.6	128	4	209	2.2	377	1.2	705
1000	4.7	127	2.9	209	1.6	377	.85	705

Table(4.3.2) Natural frequencies of clamped beams with sliding masses and initial curvature

4.4 COMPARISON AND DISCUSSION OF EXPERIMENTAL RESULTS OF CURVED CLAMPED BEAMS WITH SLIDING END MASSES

As for simply supported beam, the two natural frequencies of clamped beam with initial curvature and sliding end mass were obtained by using both theoretical and experimental analysis and are compared graphically in figures(4.4.1-4.4.10).

For the curves of first fundamental mode, the discrepancy between theoretical and experimental results was about 10%-20%.

For the curves of second fundamental mode, the discrepancy was about 15%-35%. The discrepancy increases when the initial curvature z increases or the end mass increases.

As the simply supported beam, the influences among the frequency, end mass, initial curvature and dimension of the beam were noted from the experimental and theoretical results:

(1) the natural frequency of the clamped beam tends to increase when the radius of gyration of the beam tends to increase.

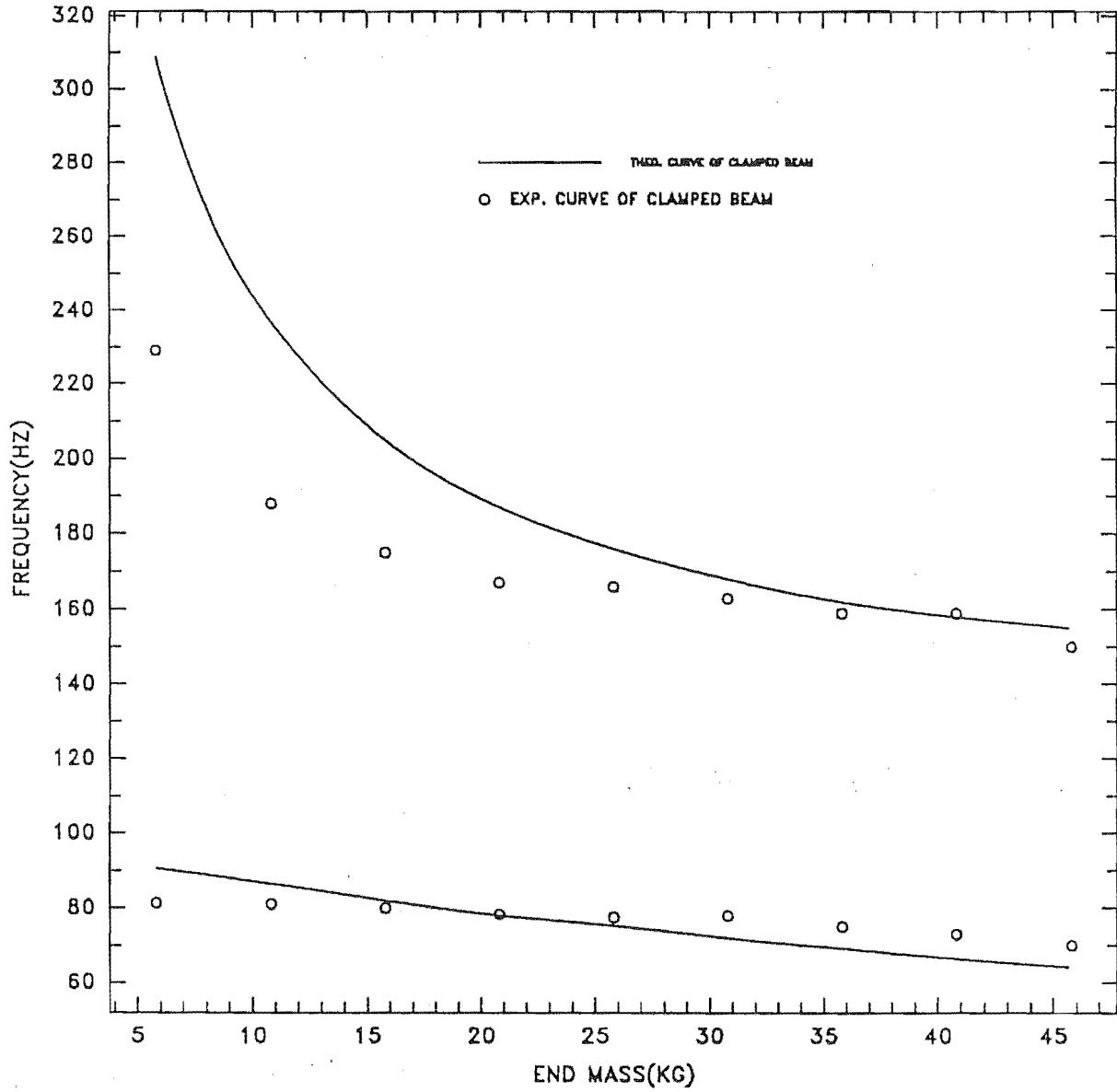
(2) For the first fundamental mode, the natural frequency of the clamped beam tends to decrease when the initial curvature z tends to increase. However the reverse

is exhibited for second fundamental mode. This can be seen from figures(4.4.1) - (4.4.10).

(3) The difference between the values of first and second fundamental natural frequencies tend to increase when the initial curvature z increase. For the 12.56x6.3x600 mm beams with end mass ($M=20\text{Kg}$), the ratio of two frequencies increase about from 1:3.4 to 1:27 when the initial curvature Z increases from 2.45 mm to 22 mm. For the 9.4 x 3 x 600 mm beam with end mass ($M=20\text{Kg}$), the ratio of two fundamental frequencies increase about from 1:5.7 to 1:34 when the initial curvature z increases from 3.1 to 19 mm as shown in figures(4.4.9) and (4.4.10).

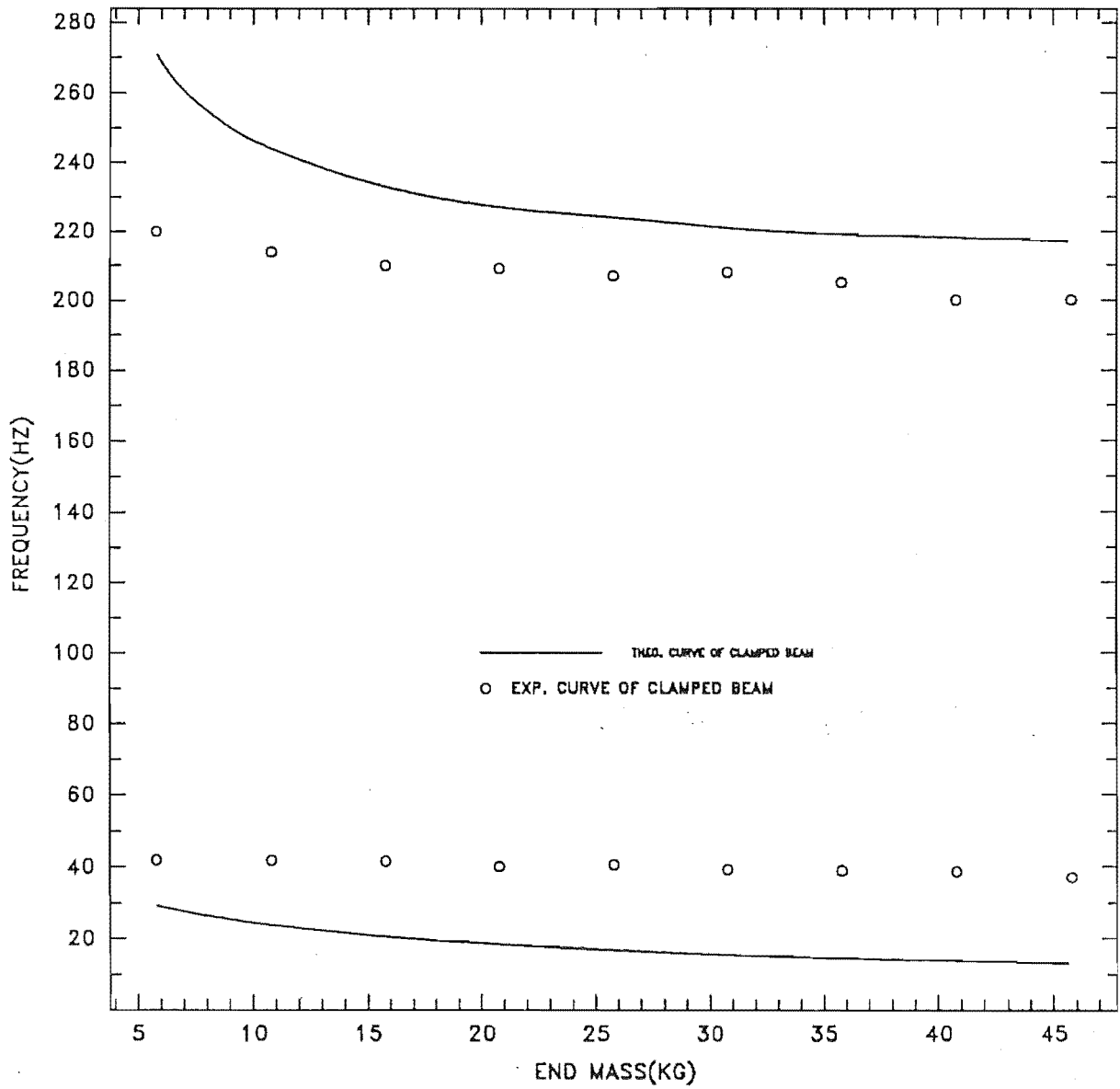
(4) For the second fundamental natural frequencies, the variation of the square of (Ω_t/Ω_0) with the square of (Z/r) is similar to that for the simply supported case.

BEAM(9.4*3.0*600mm) Z=3.10



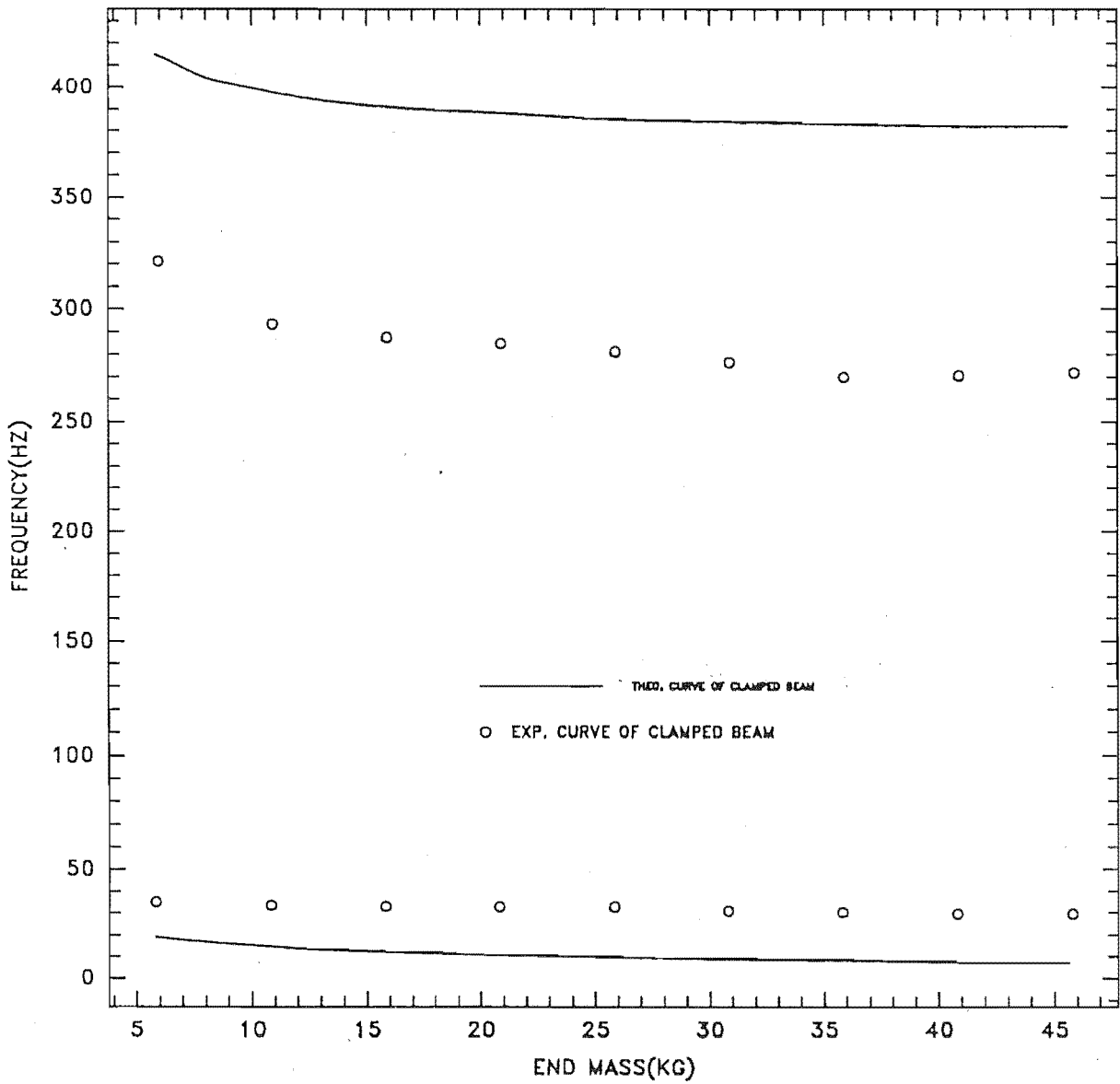
Figure(4.4.1) Frequency(Hz) of clamped beam vs. end mass(Kg)

BEAM(9.4*3.0*600mm) Z=5.5



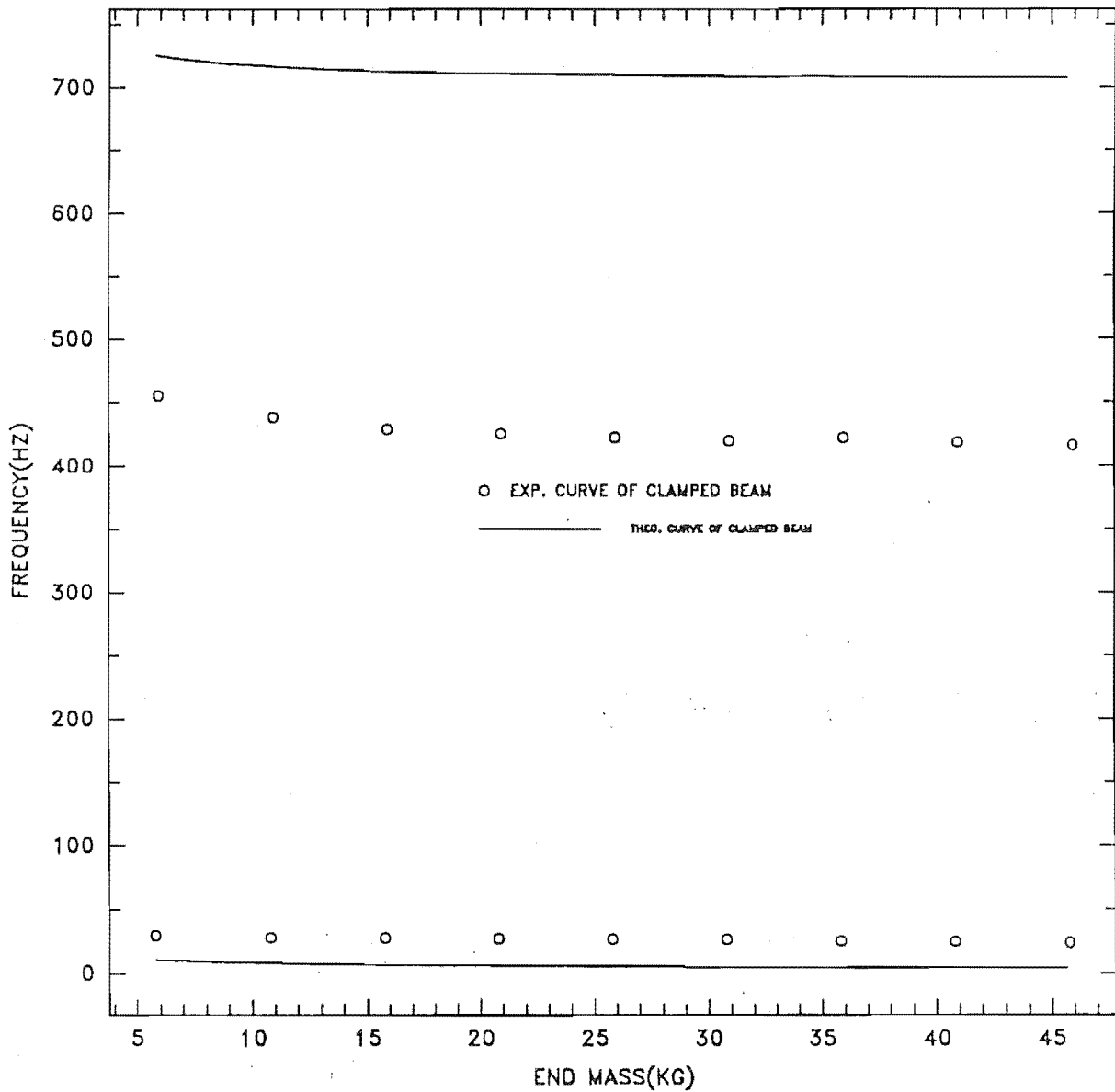
Figure(4.4.2) Frequency(Hz) of clamped beam vs. end mass(Kg)

BEAM(9.4*3.0*600mm) Z=10.10



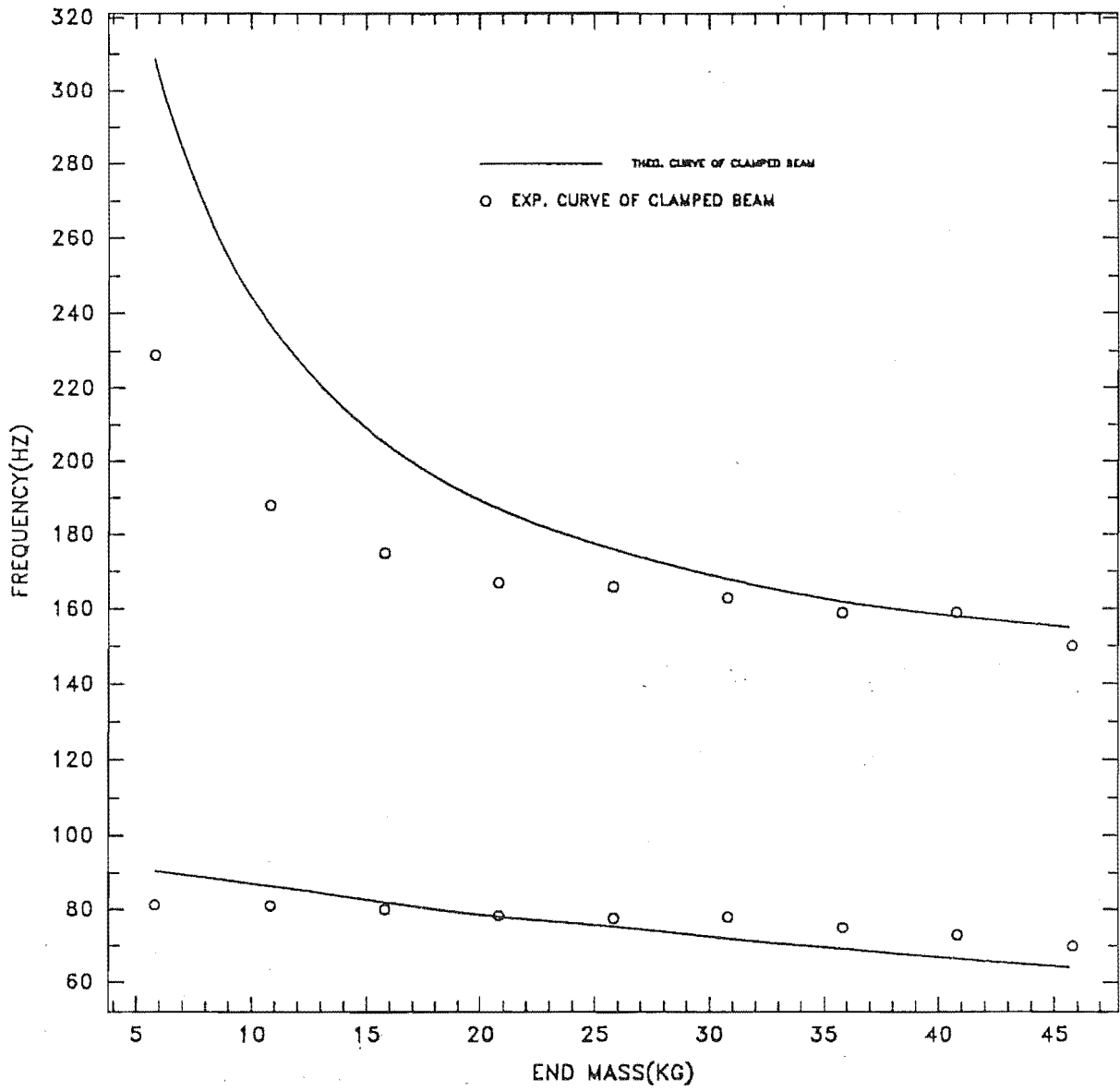
Figure(4.4.3) Frequency(Hz) of clamped beam vs. end mass(Kg)

BEAM(9.4*3.0*600mm) Z=19.00



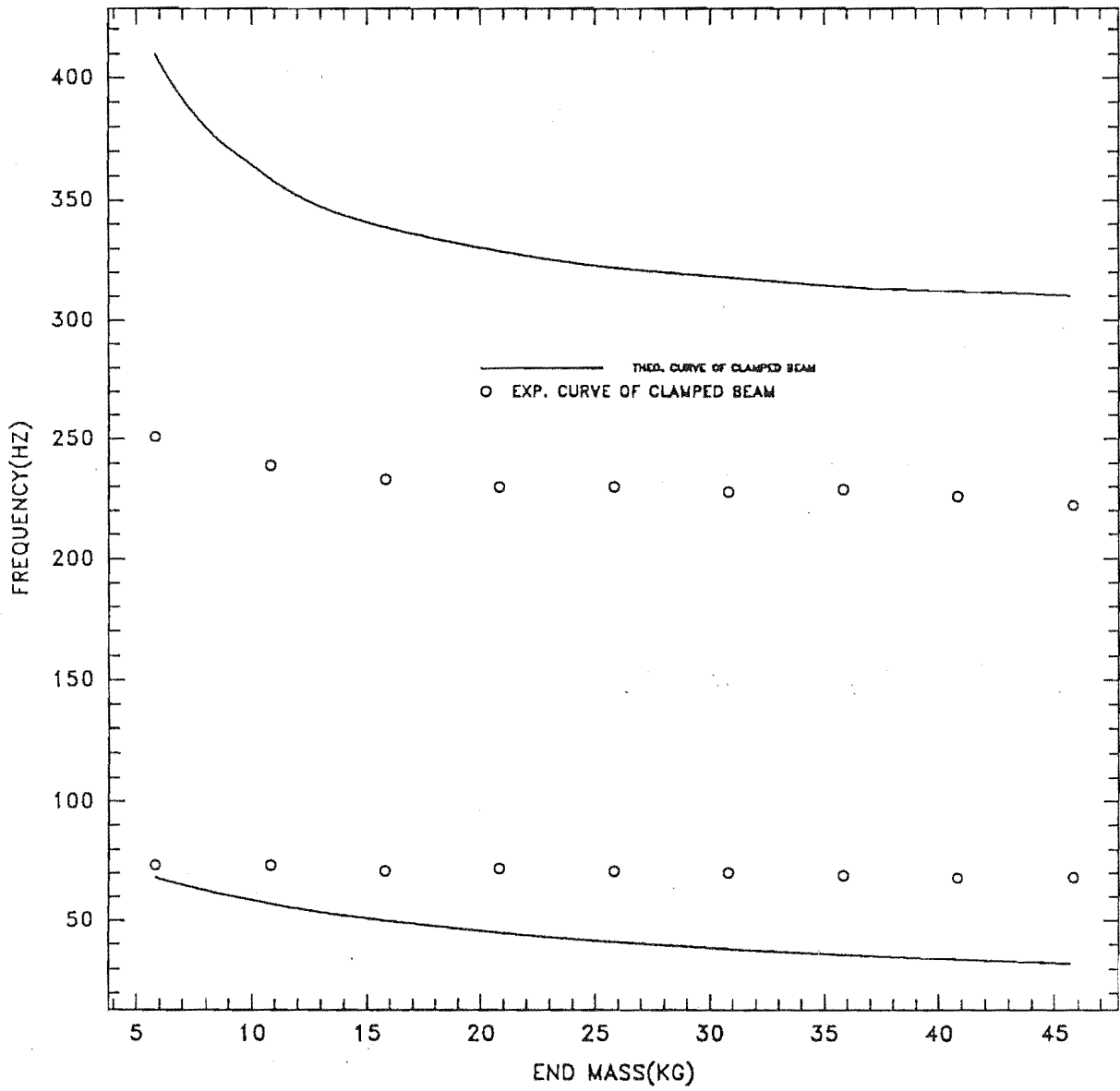
Figure(4.4.4) Frequency(Hz) of clamped beam vs. end mass(Kg)

BEAM(12.56*6.3*600mm) Z=2.45



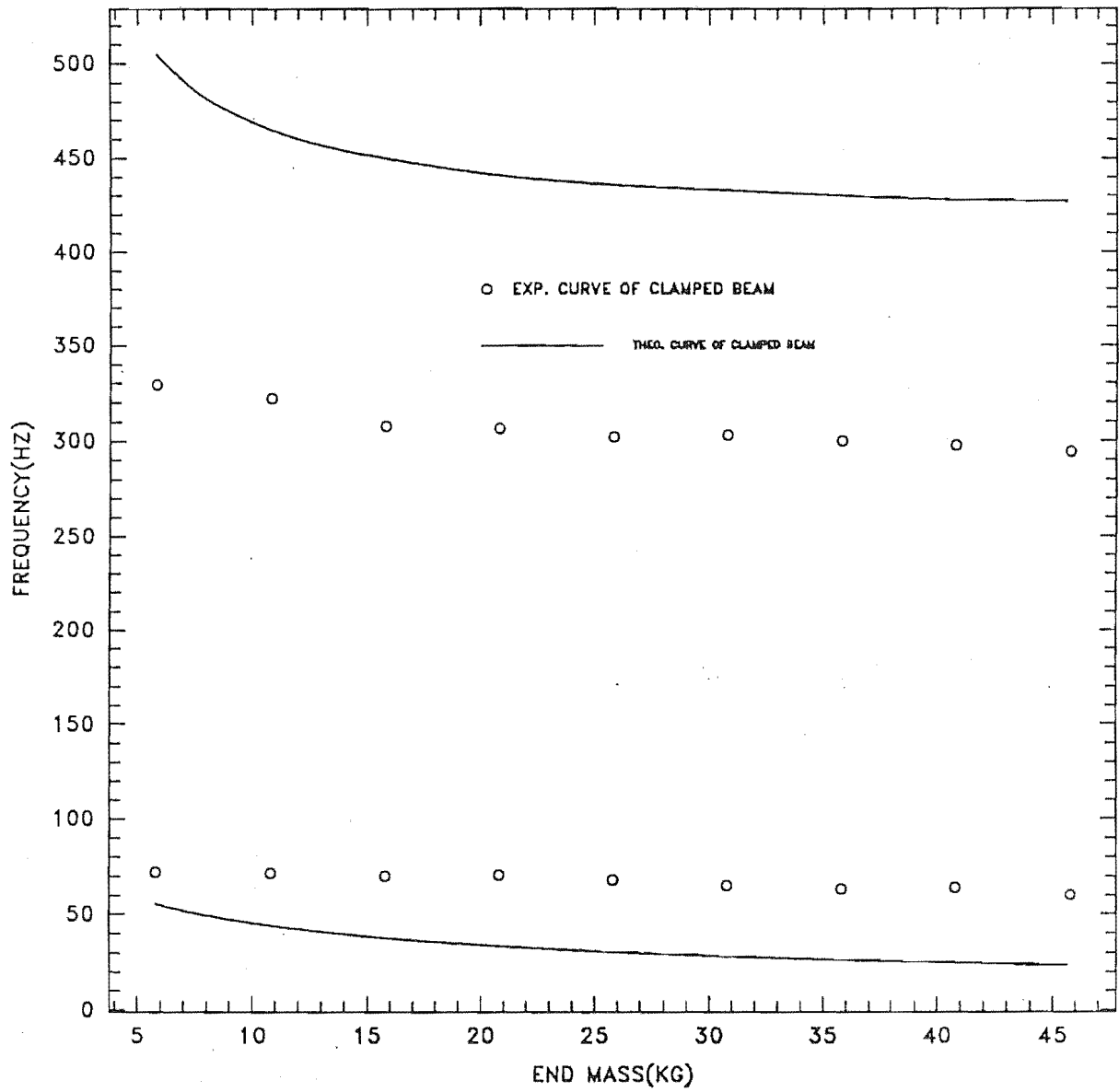
Figure(4.4.5) Frequency(Hz) of clamped beam vs. end mass(Kg)

BEAM(12.56*6.3*600mm) Z=7.00



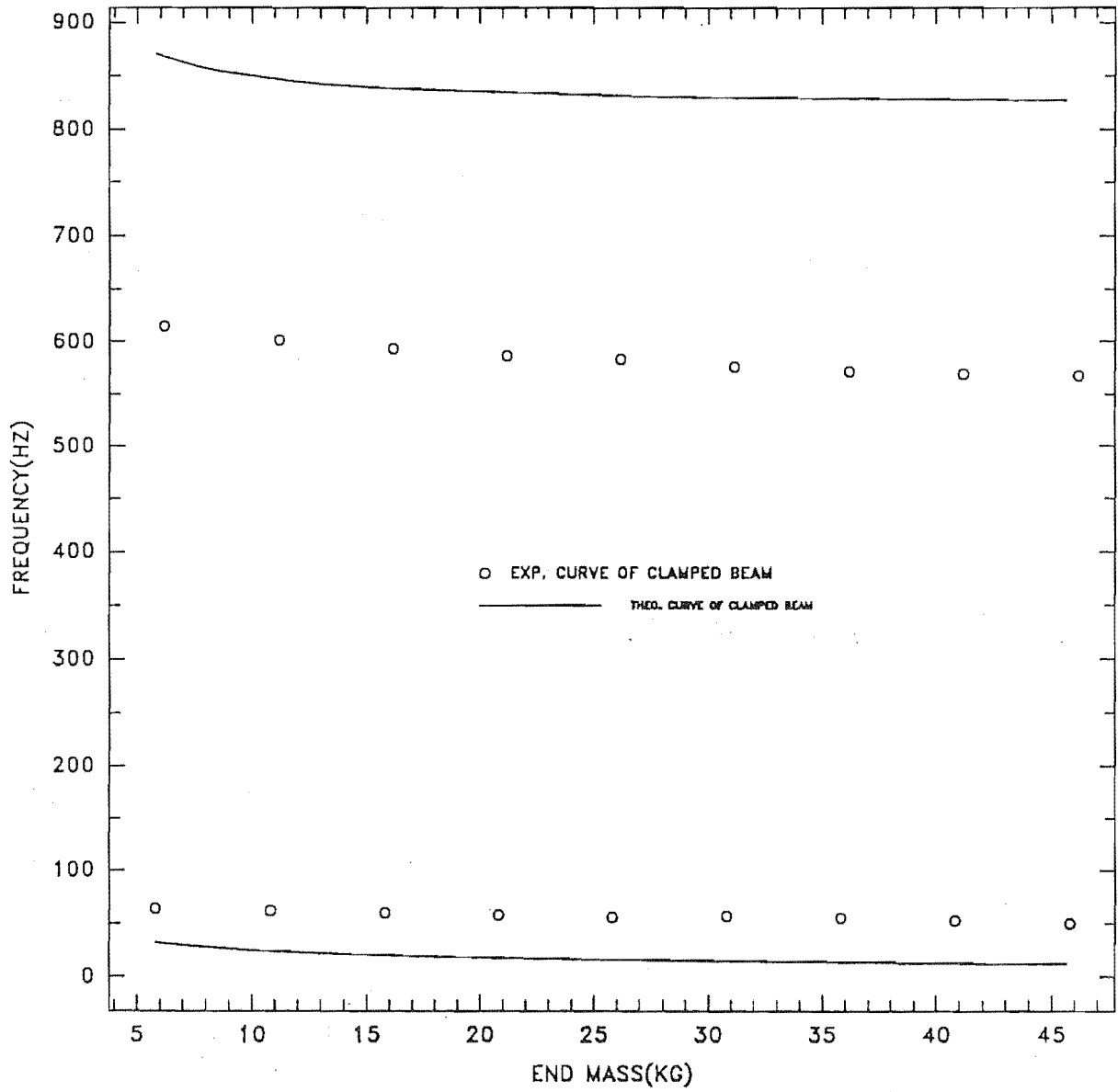
Figure(4.4.6) Frequency(Hz) of clamped beam vs. end mass(Kg)

BEAM(12.56*6.3*600mm) Z=10.90

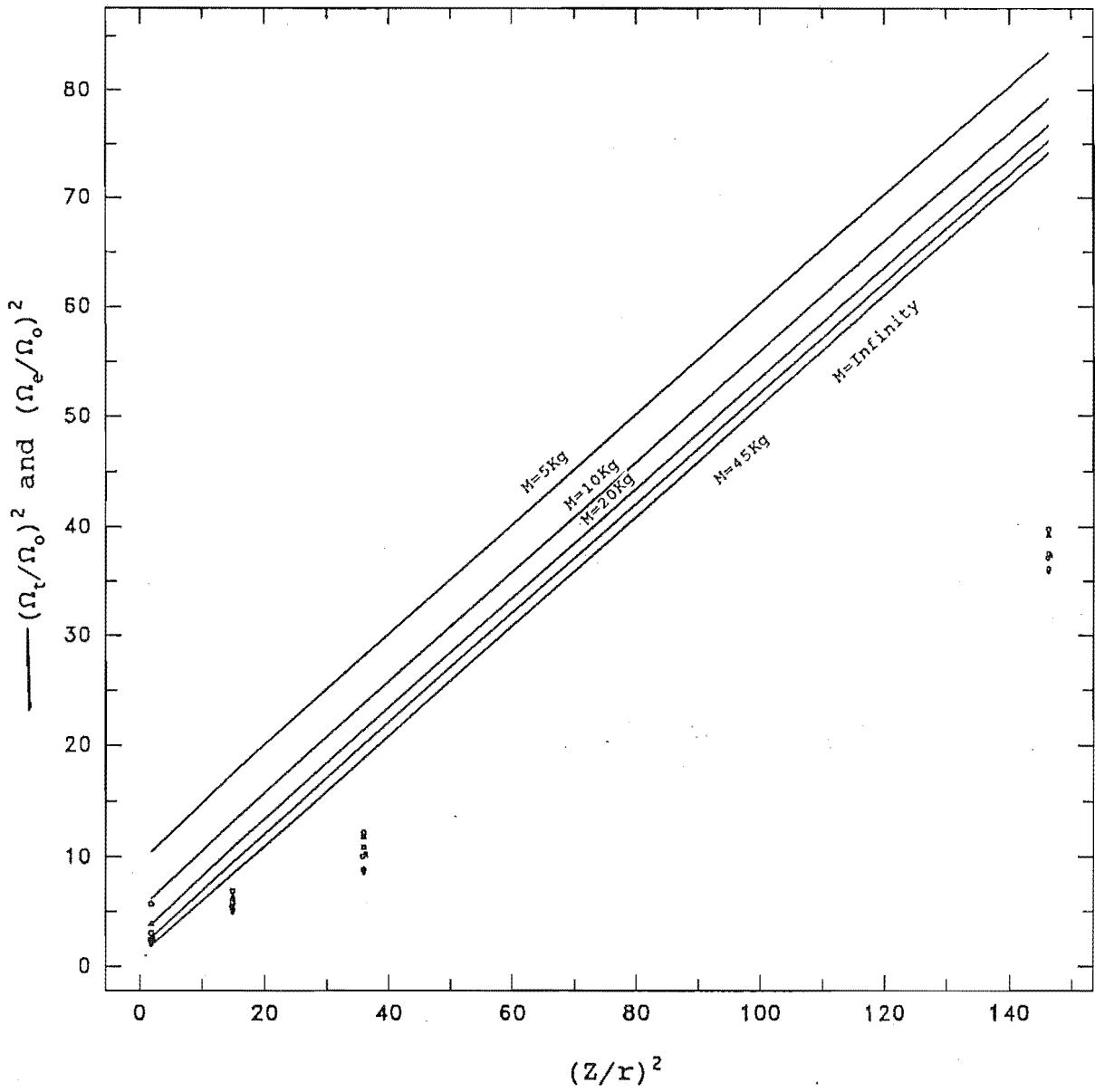


Figure(4.4.7) Frequency(Hz) of clamped beam vs. end mass(Kg)

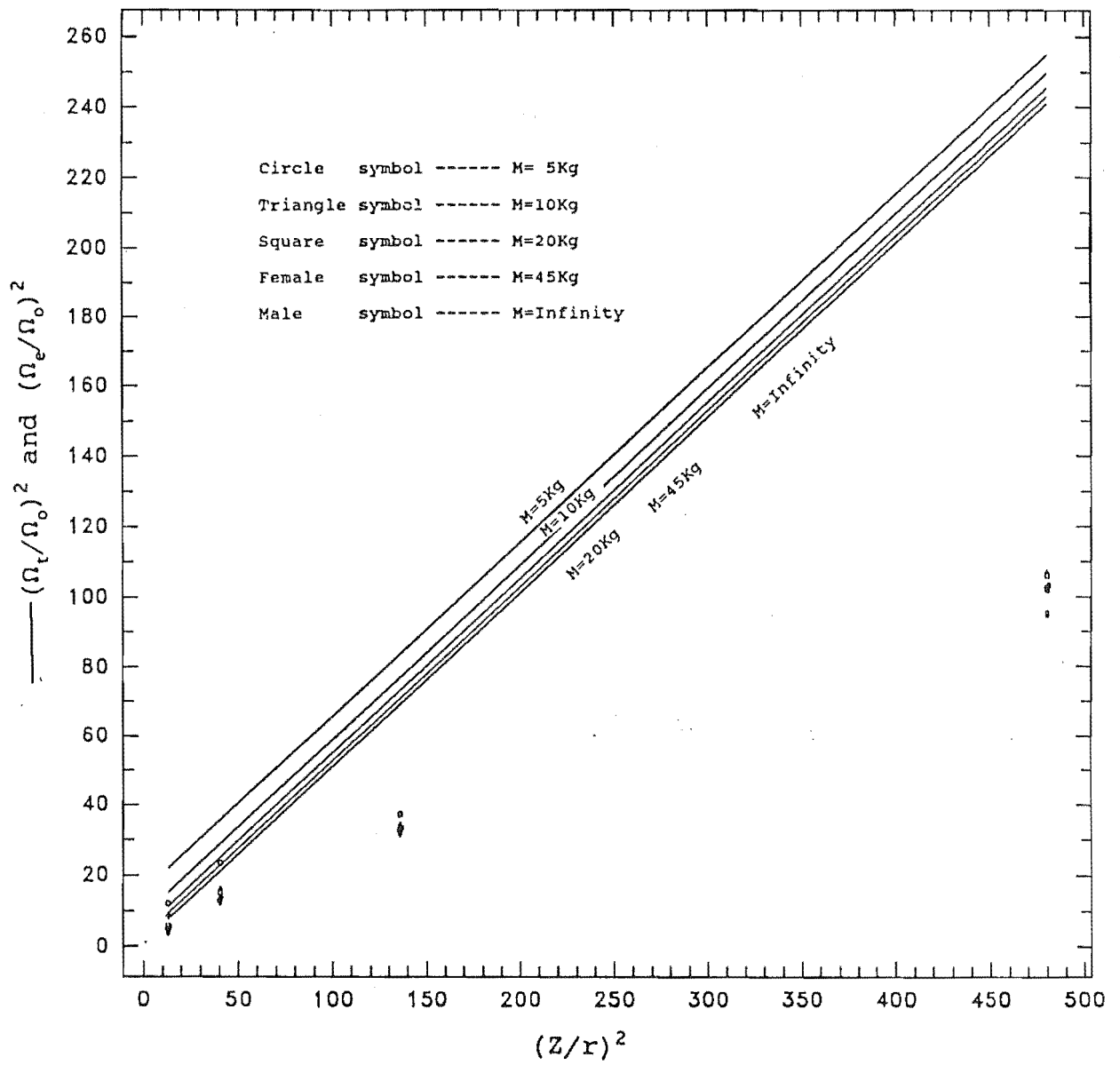
BEAM(12.56*6.3*600mm) Z=22.00



Figure(4.4.8) Frequency(Hz) of clamped beam vs. end mass(Kg)



Figure(4.4.9) $(\Omega_t/\Omega_0)^2$ and $(\Omega_e/\Omega_0)^2$ vs. $(Z/r)^2$ of clamped beam (12.56x6.3x600 mm)



Figure(4.4.10) $(\Omega_r/\Omega_0)^2$ and $(\Omega_e/\Omega_0)^2$ vs. $(Z/r)^2$ of clamped beam (9.4x3x600 mm)

From the comparison of experimental and theoretical results of clamped beam, it is noted that the agreement between them is not good compared with the agreement for the simply supported beam. In this case the effect of theoretical results calculated by including axial inertial force of the beam may be investigated to compare with the experimental results, however it is too complex to solve this problem using the same method as that used for simply supported beam as in equation(2.4.5). A better way has not been found in this project. Except this, the discrepancy may be attributed to the following factors also:

(1) The possible rotational flexibility of the support blocks. (An analysis carried out to evaluate the contribution of imperfect support condition is given in Appendix B.)

(2) Induced initial stresses due to clamping of edges on set up.

(3) Friction at ball bearings against free motion of sliding end mass in axial direction.

(4) Shape of the initial curvature of the beam being different from the assume shape. Further investigation is given in appendix A.

(5) Presence of initial residual stresses especially in those beams with large initial curvature since the beams were not stress relieved prior to testing.

(6) Measurement errors and errors due to simplifying assumptions made in modelling as explained in appendices A and C.

Although the discrepancy between the two results is considerably large, the tendency of experimental and theoretical curves is similar.

4.5 CONCLUSIONS

This thesis represents the result of an attempt to investigate the vibration behaviour of slightly curved simply supported and clamped beams with sliding end masses. The following conclusions can be reached from the discussion in the previous section:

(1) Galerkin's method has been successfully applied to calculate the natural frequencies of simply supported and clamped initially curved beams connected to axially sliding end masses. The effect of longitudinal inertia of the beam was also studied theoretically for the simply supported case.

(2) Tests were carried out on some initially curved aluminum beams of uniform sectional dimension subject to different boundary support conditions. The natural frequencies and initial geometrical imperfection were measured.

(3) The calculated and measured values of natural frequencies agree reasonably for the beam with very small initial curvatures except for small masses. However, substantial discrepancies between the theoretical and experimental results were obtained for beams with large initial curvatures.

(4) Experimental and theoretical results have shown

that:

a) There are two different natural frequencies for simply supported and clamped curved beams with axially sliding end masses corresponding to the fundamental transverse modes.

b) The presence of initial imperfection influences the natural frequencies of the beams. The frequency corresponding to first fundamental mode tends to decrease when the value of imperfection is increased. However, the reverse is exhibited for the frequency corresponding to second fundamental mode.

c) The end masses influence the natural frequencies of curved beam corresponding to fundamental mode. The frequencies tend to decrease when the masses are increased. The natural frequency of a straight beam however, is not influenced by end masses.

d) Any restraint against rotation of the beam in the end influences the natural frequency. The natural frequency increases when the restraint existing in the end of beam increases. However there was no evidence to suggest that the results for the beam tested were affected by this factor.

4.6 RECOMMENDATION FOR FUTURE WORK

The work presented in this thesis may be extended in the following areas:

1) Further investigation may be carried out to find the reason(s) for the discrepancy between the theoretical and experimental values of the fundamental natural frequencies as encountered in the present study.

2) The experimental equipment may be modified to measure the natural frequency of the beam subject to different boundary conditions other than simply supported and clamped beams.

3) This study may be extended to include the higher modes of vibration.

4) Further studies may be carried out to investigate the effect of axial inertia of clamped beam in the theoretical analysis.

5) Further research in this field may be conducted to evaluate possible practical applications.

REFERENCES

1. Plaut, R. H., "Displacement bounds for beam-columns with initial curvature subject to transient loads", International Journal of Solids and Structures, Vol. 7, No.9, 1971, pp.1229-1235.
2. Plaut, R. H. and Johnson, E. R., "The effects of initial thrust and elastic foundation on the vibration frequencies of a shallow arch", Journal of Sound and Vibration, Vol. 78, No.4, 1981, pp. 565-571.
3. Dickinson, S. M., "The lateral vibration of slightly bent slender beams subject to prescribed axial end displacement", Journal of Sound and Vibration, Vol. 68, No.4, 1980, pp. 507-514.
4. C. S. Kim, "The lateral vibration of slightly bent slender beams subject to prescribed axial end displacement" Master thesis, University of Western Ontario, Ontario, 1984.
5. M. Chi, B. G. Dennis, Jr and J. Vossoughi, "Transverse and torsional vibration of an axially loaded beam with elastically constrained ends", "Journal of Sound and Vibration", Vol.96, 1988, pp.235-241.
6. A. V. Srinivasan, "Large amplitude free oscillations of beams and plates", "American institute of Astronautics Journal", Vol 3, 1965, pp.1151-1153.

7. I. S. Raju, G. V. Rao and K. K. Raju, "Effect of longitudinal or in-plane deformation and inertia on the large amplitude flexural vibration of slender beams and thin plates", "Journal of Sound and Vibration", Vol.49, 1976, pp. 415-422.
8. K. N. Ling, "The lateral vibration of a slightly curved simply supported beam with sliding end masses", University of Canterbury. 1988.
9. M. M. Bennouna and R. G. White, "The effect of large vibration amplitudes on the fundamental mode shape of a clamped-clamped uniform beam", "Journal of Sound and Vibration", Vol.96, 1988, pp. 309-331.
10. A. Picard, D. Beaulieu and B. Perusse, "Rotational restraint of a simple column base connection", Canadian Journal of Civil Engineering", Col.14, 1976, pp.49-57.
11. S. Ilanko, "Vibration behaviour of in-plane loaded thin rectangular plates with initial geometrical imperfection", University of Western Ontario, Nov. 1988.
12. L. S. D. Morley, "Elastic waves in a natural curved rod", "Quarterly Journal of Mechanics and Applied Mathematics", Vol. 14, Pt.2, 1961, pp.155-172.
13. J.-R. Wu and W. H. Liu, "Vibration of rectangular plates with edge restraints and intermediate stiffness", "Journal of Sound and Vibration" Vol.123, No.1, 1988, pp. 103-113.

14. W. H. Liu and C.-C. Huang, "Vibration of a constrained beam carrying a heavy tip body", "Journal of Sound and Vibration", Vol.123, No.1, 1988, pp. 15-29.

15. I. G. Currie and Cleghorn, "Free lateral vibration of a beam under tension with a concentrated mass at the mid-point", "Journal of Sound and Vibration", Vol.123, No.1, 1988, pp. 55-61.

16. H. McCallion, "Vibration of linear mechanical systems", University of Canterbury.

17. R. P. Goel, "Free vibrations of a beam-mass system with elastically restrained ends", "Journal of Sound and Vibration", Vol.123, No.47, pp. 9-14.

Appendix A

THEORETICAL ANALYSIS OF THE CURVATURE OF THE SIMPLY SUPPORTED BEAM

In the previous analysis work, the curvature of the simply supported beam was taken as sine function $Y_0 = Z \sin(\pi X/L)$. However, it would be very difficult to make such a curvature of the beam which may agree with sine function $Y_0 = Z \sin(\pi X/L)$ perfectly along the axial direction of the beam. Using measuring and theoretical method may obtain more accurate results as show below:

the initial curvatures of the beam may be taken as a Fourier Series

$$Y_0(X) = Z_1 \sin(\pi X/L) + Z_2 \sin(2\pi X/L) + Z_3 \sin(3\pi X/L) + Z_4 \sin(4\pi X/L) + \dots + Z_m \sin(m\pi X/L) \quad (A.1)$$

Where $Z_1, Z_2, Z_3, \dots, Z_m$ are coefficients of the function of Fourier Series.

Applying Galerkin's method to equation (A.1) using $Y_j = \sin(n\pi X/L)$ as weighting function gives,

$$\int_0^L Y_0(X) \sin(\pi X/L) dX = Z_1 \int_0^L \sin(\pi X/L) \sin(\pi X/L) dX + Z_2$$

$$\int_0^L \sin(2\pi X/L) \sin(n\pi X/L) dX + \dots + Z_m \int_0^L \sin(m\pi X/L) \sin(n\pi X/L) dX \quad (A.2)$$

(n, m=1, 2, \dots, \infty)

Let $Y_n(X) \sin(n\pi X/L) = P_n(X)$

If n=1 equation (A.2) becomes,

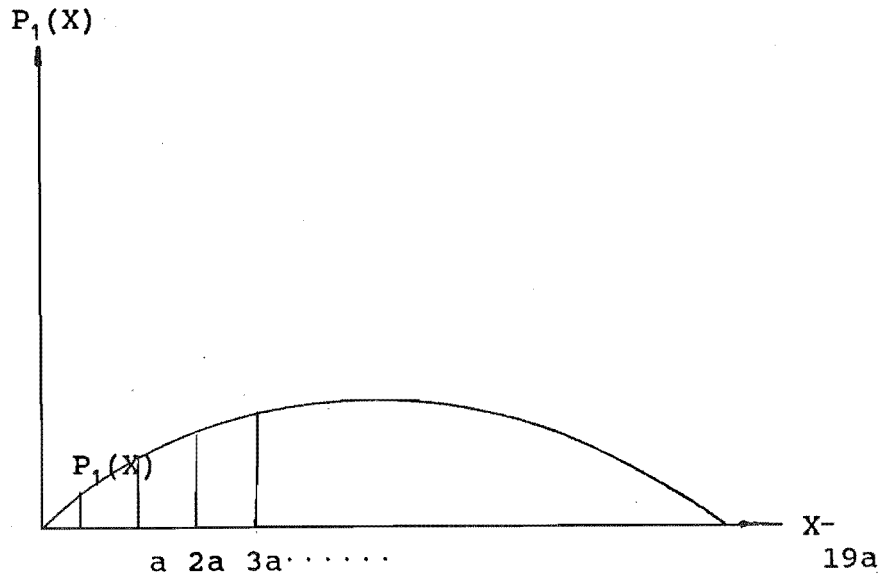
$$\int_0^L Y_1(X) \sin(\pi X/L) dX = Z_1 \int_0^L \sin^2(\pi X/L) dX + Z_2 \int_0^L \sin(2\pi X/L) \sin(\pi X/L) dX + \dots + Z_m \int_0^L \sin(m\pi X/L) \sin(\pi X/L) dX$$

$$\int_0^L P_1(X) dX = Z_1 \int_0^L \sin^2(\pi X/L) dX$$

$$\int_0^L P_1(X) dX = Z_1 L/2$$

The results of $\int_0^L P_1(X) dX$ may be obtained by using

measuring method as show below,



The areas of $P_1(X) = aP_1(a)/2 + a[P_1(a)+P_1(2a)]/2 +$
 $+ a[P_1(2a)+P_1(3a)]/2 + \dots + aP_1\{[(m-1)a]+P_1(ma)\}/2$

$$P_1(X) = aP_1(a) + aP_1(2a) + \dots + aP_1(ma)$$

In this project $n=19$, $a=600/(n+1)=30$ mm

$$Z_1 = (2 \times \text{Area } 1) / L$$

As the same as above equation,

$$Z_2 = (2 \times \text{Area } 2) / L, \quad Z_n = (2 \times \text{Area } n) / 2$$

The curvature of test piece (1) - (16) may be taken as $Y_1(X), Y_2(X) \dots Y_{16}(X)$. Calculating by computer program, $Z_1, Z_2 \dots Z_5$ were obtained as showed below,

$$Y_1(X) = 2.81719 \sin(\pi X/L) + (-0.1007) \sin(2\pi X/L) +$$

$$0.243 \sin(3\pi X/L) + 0.00266 \sin(4\pi X/L) + (-0.003014) \sin(5\pi X/L)$$

$$Y_2(X) = 7.0314 \sin(\pi X/L) + 0.176 \sin(2\pi X/L) + 0.235 \sin(3\pi X/L) + (-0.02889) \sin(4\pi X/L) + 0.1671 \sin(5\pi X/L)$$

$$Y_3(X) = 11.046 \sin(\pi X/L) + 0.429 \sin(2\pi X/L) + 0.168 \sin(3\pi X/L) + 0.0026 \sin(4\pi X/L) + (-0.0565) \sin(5\pi X/L)$$

$$Y_4(X) = 22.5511 \sin(\pi X/L) + (-7.9 \times 10^{-3}) \sin(2\pi X/L) + 0.879 \sin(3\pi X/L) + 0.2028 \sin(4\pi X/L) + 0.4500 \sin(5\pi X/L)$$

$$Y_5(X) = 3.1003 \sin(\pi X/L) + 0.123 \sin(2\pi X/L) + 0.212 \sin(3\pi X/L) + 0.145 \sin(4\pi X/L) + 0.2001 \sin(5\pi X/L)$$

$$Y_6(X) = 5.522 \sin(\pi X/L) + (-0.128) \sin(2\pi X/L) + 0.432 \sin(3\pi X/L) + 0.212 \sin(4\pi X/L) + 0.328 \sin(5\pi X/L)$$

$$Y_7(X) = 10.182 \sin(\pi X/L) + (-6.8 \times 10^{-3}) \sin(2\pi X/L) + 0.823 \sin(3\pi X/L) + 0.386 \sin(4\pi X/L) + 0.142 \sin(5\pi X/L)$$

$$Y_8(X) = 19.1834 \sin(\pi X/L) + (-5.2 \times 10^{-2}) \sin(2\pi X/L) + 0.328 \sin(3\pi X/L) + 0.110 \sin(4\pi X/L) + 0.1001 \sin(5\pi X/L)$$

$$Y_9(X) = 2.723 \sin(\pi X/L) + (-0.0992) \sin(2\pi X/L) + 0.198 \sin(3\pi X/L) + 0.02543 \sin(4\pi X/L) + (-0.00298) \sin(5\pi X/L)$$

$$Y_{10}(X) = 7.0833 \sin(\pi X/L) + 0.1798 \sin(2\pi X/L) + 0.23887 \sin(3\pi X/L) + (-0.02987) \sin(4\pi X/L) + 0.16832 \sin(5\pi X/L)$$

$$Y_{11}(X) = 10.978 \sin(\pi X/L) + 0.4132 \sin(2\pi X/L) + 0.1712 \sin(3\pi X/L) + 0.4432 \sin(4\pi X/L) + (-0.00543) \sin(5\pi X/L)$$

$$Y_{12}(X) = 22.543 \sin(\pi X/L) + (-8.54 \times 10^{-3}) \sin(2\pi X/L) + 0.899 \sin(3\pi X/L) + 0.3100 \sin(4\pi X/L) + 0.4467 \sin(5\pi X/L)$$

$$Y_{13}(X) = 2.9987 \sin(\pi X/L) + 0.176 \sin(2\pi X/L) +$$

$$0.20013\sin(3\pi X/L) + 0.1445\sin(4\pi x/L) + 0.1912\sin(5\pi X/L)$$

$$Y_{14}(X) = 5.523\sin(\pi X/L) + (-0.1923)\sin(2\pi X/L) + \\ 0.457\sin(3\pi X/L) + 0.233\sin(4\pi x/L) + 0.345\sin(5\pi X/L)$$

$$Y_{15}(X) = 10.173\sin(\pi X/L) + (-6.33 \times 10^{-3})\sin(2\pi X/L) + \\ 0.732\sin(3\pi X/L) + 0.455\sin(4\pi x/L) + 0.1009\sin(5\pi X/L)$$

$$Y_{16}(X) = 19.1882\sin(\pi X/L) + (-9.87 \times 10^{-3})\sin(2\pi X/L) + \\ 0.361\sin(3\pi X/L) + 0.109\sin(4\pi x/L) + 0.0993\sin(5\pi X/L)$$

In chapter 4, the discussion will be done to compare with the initial curvatures of the simply supported beam taken as sine function $Y = Z\sin(\pi X/L)$ and taken as Fourier Series

$$Y_a(X) = Z_1 \sin(\pi X/L) + Z_2 \sin(2\pi X/L) + Z_3 \sin(3\pi X/L) + \\ Z_4 \sin(4\pi X/L) + \dots + Z_m \sin(m\pi X/L).$$

Appendix B

THE EFFECT OF ROTARY INERTIA OF THE END MASSES

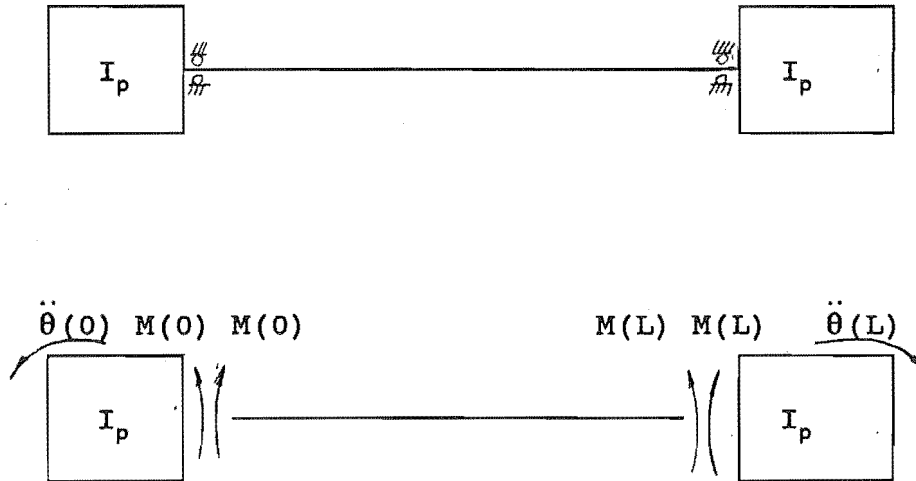


Figure (B.1) Free end mass diagram subject to rotary inertia

Consider the beam vibration equation

$$\partial^4 Y / \partial X^4 + m \partial^2 Y / \partial t^2 = 0$$

The transverse dynamic displacement $Y(X)$ of the beam may be

taken as a general solution of the beam vibration equation.

$$y(x, t) = Y(x) \sin(\omega t + \alpha)$$

Where $Y(x)$ is as follows

$$Y(x) = G_1 \cosh(\lambda x / L) + G_2 \sinh(\lambda x / L) + G_3 \cos(\lambda x / L) + G_4 \sin(\lambda x / L)$$

(B.1)

Where G_1, G_2, G_3, G_4 is a constant of integration.

Consider the boundary condition of the rotating masses at both ends. From the basic theory of beam bending equation $M=EI\partial^2Y/\partial X^2$, gives,

$$M(0)=I_p\theta(0)=EI\partial^2Y(0)/\partial X^2=-\omega^2I_p\theta(0)=-\omega^2I_pY'(0)$$

$$M(L)=-I_p\theta(L)=EI\partial^2Y(L)/\partial X^2=\omega^2I_p\theta(L)=\omega^2I_pY'(L)$$

(a) At $X=0$, $y=0$ ie $Y(0)=0$ substitute into equation(B.1)

$$G_1x1.0+G_2x1.0+G_3x1.0+G_4x1.0=0 \quad (B.2)$$

(b) At $x=0$, $M(0)=I_p\theta(0)=EI\partial^2Y(0)/\partial X^2=-\omega^2I_p\theta(0)=-\omega^2I_pY'(0)$

gives,

$$-\omega^2I_pY_x/EI=\partial^2Y/\partial X^2$$

$$G_1(\lambda/L)-G_3(\lambda/L)+G_2\omega^2I_p/EI+G_4\omega^2I_p/EI = 0 \quad (B.3)$$

(c) At $x=L$, $y=0$

$$Y(L)=0$$

$$G_1\cosh\lambda+G_2\sinh\lambda+G_3\cos\lambda+G_4\sin\lambda = 0 \quad (B.4)$$

(d) At $x=L$,

$$M(L)=I_p\theta(L)=EI\partial^2Y(L)/\partial X^2=-\omega^2I_p\theta(L)=-\omega^2I_pY'(L)$$

gives,

$$\omega^2I_pY_x(L)/EI=\partial^2Y(L)/\partial X^2$$

$$\text{As } Y_x(L)=(\lambda/L)[G_1\sinh\lambda+G_2\cosh\lambda-G_3\sin\lambda+G_4\cos\lambda] = 0$$

$$Y_{xx}(L)=(\lambda/L)[G_1\cosh\lambda+G_2\sinh\lambda-G_3\cos\lambda-G_4\sin\lambda] = 0$$

gives,

$$G_1[(\omega^2I_p\sinh\lambda)/EI-(\lambda/L)\cosh\lambda] + G_2[(\omega^2I_p\cosh\lambda)/EI-(\lambda/L)\sinh\lambda] - G_3[(\omega^2I_p\sin\lambda)/EI-(\lambda/L)\cos\lambda] + G_4[(\omega^2I_p\cos\lambda)/EI+(\lambda/L)\sin\lambda] = 0 \quad (B.5)$$

The equation(B.2) - (B.5) may be written in matrix form

$$\text{as } [C]\{G\} = 0$$

Where

$$C_{11}=1.0 \quad C_{12}=0 \quad C_{13}=1.0 \quad C_{14}=0$$

$$C_{21}=\lambda/L \quad C_{22}=\omega^2 I_p/EI \quad C_{23}=-\lambda/L \quad C_{24}=\omega^2 I_p/EI$$

$$C_{31}=\cosh\lambda \quad C_{32}=\sinh\lambda \quad C_{33}=\cos\lambda \quad C_{34}=\sin\lambda$$

$$C_{41}=(\omega^2 I_p \sinh\lambda)/EI - (\lambda/L) \cosh\lambda$$

$$C_{42}=(\omega^2 I_p \cosh\lambda)/EI - (\lambda/L) \sinh\lambda$$

$$C_{43}=(\omega^2 I_p \sin\lambda)/EI + (\lambda/L) \cos\lambda$$

$$C_{44}=(\omega^2 I_p \cos\lambda)/EI - (\lambda/L) \sin\lambda$$

For non-trivial solution of $\{C\}$, determine $[C]=0$. This is the characteristic equation. Instituting $(\lambda/L)^4 = m\omega^2/EI$ into matrix $[C]=0$, the equation may be obtained as follows,

$$\begin{aligned} & [(\lambda/L)^4 I_p \sinh\lambda/m - (\lambda/L) \cosh\lambda] [(-\lambda/L)^4 I_p \sinh\lambda/m + (\lambda/L)^4 I_p \sin\lambda/m] + \\ & [(\lambda/L)^4 I_p \cosh\lambda/m - (\lambda/L) \sinh\lambda] [-(2\omega/l) \sin\lambda + (\lambda/L)^4 I_p \cosh\lambda/m - \\ & (\lambda/L)^4 I_p \cos\lambda/m] - \\ & [-(\lambda/L)^4 I_p \sin\lambda/m + (\lambda/L) \cos\lambda] [(\lambda/L)^4 I_p \sin\lambda/m - (\lambda/L)^4 I_p \sinh\lambda/m] + \\ & [(\lambda/L)^4 I_p \cos\lambda/m + (\lambda/L) \sin\lambda] [(\lambda/L)^4 I_p \cos\lambda/m - (\lambda/L)^4 I_p \cosh\lambda/m] \\ & = 0 \end{aligned} \quad (B.7)$$

Using try method, the solution can be obtained by computer program as follows,

Table(B.1) The results of equation(B.7)

M(Kg)	I_p (Kg m ⁴)	λ_1	λ_2	ω_1 (Hz)	ω_2 (Hz)
0	0	3.16	6.4	40.8	163.2
2	.0005	3.5	7	48.82	195.28
5.8	.00673	3.8	7.6	57.55	230.2
10.8	.0169	4.1	8.2	66.9	267.6
15.8	.0274	4.3	8.6	73.6	294.4
20.8	.0406	4.4	8.8	77.15	308.6
25.8	.0579	4.49	8.98	80.7	322.8
30.8	.0805	4.58	9.16	84.3	337.2
35.8	.1099	4.67	9.34	88.03	352.1
40.8	.1463	4.70	9.40	88.4	353.6
45.8	.1915	4.71	9.42	89.1	356.4
∞		4.73	9.46	89.9	359.6

Appendix C

ERROR ANALYSIS

The natural frequency may be influenced by the factors including E, I, m, L, Z etc. In this chapter, measuring errors of initial curvature Z, length of beam L and Young's modulus E errors between the tested beam and standard aluminium are investigated. The equations (C.1-C.6) may present these effects shown below,

The natural frequency could be given,

$$\Omega = F(E, I, m, L, Z \dots\dots\dots)$$

Rearranging equation(2.2.10) gives,

$$2r^2ML\Omega^4 - (4r^2EA + 2r^2ML\Omega_0^2 + Z^2ML\Omega_0^2)\Omega^2 + 4r^2EA\Omega_0^2 = 0$$

Let $X = \Omega^2$ gives,

$$2r^2MLX^2 - (4r^2EA + 2r^2ML\Omega_0^2 + Z^2ML\Omega_0^2)X + 4r^2EA\Omega_0^2 = 0$$

The error could be taken as,

$$\delta X = \frac{\partial X}{\partial Z} \delta Z + \frac{\partial X}{\partial E} \delta E + \frac{\partial X}{\partial I} \delta I + \frac{\partial X}{\partial m} \delta m + \frac{\partial X}{\partial L} \delta L \dots\dots\dots$$

1) Considering the measuring error of Z. If

$$\delta Z = 2\text{mm} (Z = 22\text{mm}, M = 5.8\text{Kg}) \text{ gives,}$$

$$\delta Z / Z = 0.09$$

$$\delta X = \frac{\partial X}{\partial Z} \delta Z$$

$$= \left(\frac{Z\Omega_0^2}{2r^2} \right) 0.09Z + \frac{0.09Z^2\Omega_0^2(4r^2EA+2r^2ML\Omega_0^2+Z^2ML\Omega_0^2)}{2r^2\sqrt{(4r^2EA+2r^2ML\Omega_0^2+Z^2ML\Omega_0^2)^2-32r^4MLEA\Omega_0^2}}$$

$$= 576, 2.281$$

$$\frac{\delta\Omega_1}{\Omega} = \frac{1.51}{26.3} = 5.7\% \quad (C.1)$$

$$\frac{\delta\Omega_2}{\Omega} = \frac{24}{461} = 5.2\% \quad (C.2)$$

2) Considering measuring and mounting errors of L. If $\delta L = 0.012$ ($Z=22\text{mm}$, $M=5.8\text{Kg}$) gives,

$$\delta L/L = 0.02$$

$$\delta X = \frac{\partial X}{\partial L} \delta L = 2590.81, 4.708$$

$$\frac{\delta\Omega_1}{\Omega} = \frac{2.17}{26.3} = 8.2\% \quad (C.3)$$

$$\frac{\delta\Omega_2}{\Omega} = \frac{50.9}{461} = 11\% \quad (C.4)$$

3) Considering the error between the Young's Modulus and tested beam. If $\delta E = 72.25 \times 10$ ($Z=22\text{mm}$, $M=5.8$) gives,

$$\delta E/E = 0.03$$

$$\delta X = \frac{\partial X}{\partial E} \delta E = 41.08, 0.1324$$

$$\frac{\delta\Omega_1}{\Omega} = \frac{0.34}{26.3} = 1.2\% \quad (\text{C.5})$$

$$\frac{\delta\Omega_2}{\Omega} = \frac{6.41}{461} = 1.3\% \quad (\text{C.6})$$

Appendix D

LIST OF COMPUTER PROGRAM

_MECHMA\$DURO:USERS.STUDENT.ZHOUJCI.FOR;52

```
PROGRAM C1
RO=2770.0
B=.0094
H=.003
Z=0.0055
GOTO 42

WRITE(*,10)
10  FORMAT(1X,'INPUT R=?')
    READ (*,*) B
    WRITE(*,20)
20  FORMAT(1X,'INPUT H=?')
    READ (*,*) H
    WRITE(*,30)
30  FORMAT(1X,'INPUT Z=?')
    READ (*,*) Z
    WRITE(*,40)
40  FORMAT(1X,'INPUT RO=?')
    READ(*,*) RO
42  WRITE(*,45)
45  FORMAT(1X,'INPUT PM=?')
    READ(*,*) PM
    A=B*H
    PI=B*H*H*H/12.0
    WRITE(*,*) 'PI=',PI
    WRITE(*,*) 'A=',A
    R=SQRT(PI/A)
    PLM=0.6*A*B*H*RO
    PSM=PLM/0.6
    E=75.0E+9
    WS=3.14*3.14*SQRT(R*A*PI*AIG/PSM/3)/0.6/0.6
    WRITE(*,*) 'WS=',WS
    WS1=SQRT(WS*WS+B*Z*Z*(3.14**4)*E*A/3/PSM/(0.6**4))
    WRITE(*,*) 'WS1=',WS1

WRITE(*,*) 'ST',SQRT(B*A*A*E*Z*Z/3/PSM)*3.14*3.14/.36
```

C

```

A1=3*PM*PSM*(0.6**4)/E/A/2
A2=-(3*PSM*(0.6**3)+4*Z*Z*(3.14**4)*PM+8*PM*(3.14**4)*PI/A)
A3=16*(3.14**4)*E*PI/0.6
WRITE(*,*)'A1=',A1
WRITE(*,*)'A2=',A2
WRITE(*,*)'A3=',A3
WRITE(*,*)'A2*A2-4*A1*A3=',(A2*A2-4*A1*A3)
X1=(-A2+SQRT(A2*A2-4*A1*A3))/2/A1
X2=(-A2-SQRT(A2*A2-4*A1*A3))/2/A1
WRITE(*,*)'X1=',X1
WRITE(*,*)'X2=',X2
IF(X1.GT.0.0) F1=SQRT(X1)
IF(X2.GT.0.0) F2=SQRT(X2)
WRITE(*,*) X1/6.28
C50  FORMAT(1X,'X1=?')
WRITE(*,*) X2/6.28
C60  FORMAT(1X,'X2=?')
WRITE(*,*) F1/6.28
C70  FORMAT(1X,'F1=?')
WRITE(*,*) F2/6.28

```

```
PROGRAM F1
REAL*16 Y,Y1,P,Q
COMPLEX X1,X2,Y2,Y3,S1,S2,S3,G1,G2,G3,YY
E=75.0D+9
RO=2770.
BB=.0125
HH=.006
WRITE(*,5)
5 FORMAT(1X,'INPUT M=' )
READ(*,*)M
WRITE(*,7)
7 FORMAT(1X,'INPUT Z=' )
READ(*,*)Z
PSM=BB*HH*RO
AA=BB*HH
PI=BB*HH*3/12.0
A1=(PSM*M*.6*RO/2/E**2/AA)
A22=-3.14**4*Z**2*M*RO/2/.6**3/E-PI*3.14**4*M*RO/2/.6**3/AA/E
A33=PSM*RO/E-2*PSM*M*3.14**2/.6/E/AA
A2=A22+A33
A44=RO*PI*3.14**4/.6**4+2*PI*3.14**6*M/AA/.6**5
A55=3.14**6*Z**2*M/.6**5+4*PSM*3.14**2/.6**2-2*PSM
A3=(A44+A55)
A4=(-4*E*PI*3.14**6/.6**6+2*E*PI*3.14**4/.6**4)
A=A2/A1
B=A3/A1
C=A4/A1
WRITE(*,*)A,B,C
X1=CMPLX(-.5,1.73/2)
X2=CMPLX(-.5,-1.73/2)
P=-A**2/3+B
Q=2*AA*3/27-A*B/3+C
WRITE(*,*)P,Q
Y=(Q/2)**2+(P/3)**3
WRITE(*,*)Y
YY=Y*(10.D-31)
Y1=(10.D+14)*SQRT(YY)
Y2=(-Q/2+Y1)**(1./3.)
Y3=(-Q/2-Y1)**(1./3.)
S1=Y2+Y3
S2=X1*Y2+X2*Y3
S3=X2*Y2+X1*Y3
G1=S1-A/3
G2=S2-A/3
G3=S3-A/3
WRITE(*,*)G1
WRITE(*,*)G2
WRITE(*,*)G3
W1=G1
W2=G2
W3=G3
IF (W1.GT.0.0) W11=SQRT(W1)
IF (W2.GT.0.0) W22=SQRT(W2)
IF (W3.GT.0.0) W33=SQRT(W3)
WRITE(*,*)W11/6.28
WRITE(*,*)W22/6.28
WRITE(*,*)W33/6.28
STOP
```

```

PROGRAM S1
RO=2770.0
B=.01256
H=.0063
Z=0.032
GOTO 42

WRITE(*,10)
10  FORMAT(IX,'INPUT B=?')
    READ (*,*) B
    WRITE(*,20)
20  FORMAT(IX,'INPUT H=?')
    READ (*,*) H
    WRITE(*,30)
30  FORMAT(IX,'INPUT Z=?')
    READ (*,*) Z
    WRITE(*,40)
40  FORMAT(IX,'INPUT RO=?')
    READ(*,*) RO
42  WRITE(*,45)
45  FORMAT(IX,'INPUT PM=?')
    READ(*,*) PM
    A=B*H
    PI=B*H*H*H/12.0
        WRITE(*,*)'PI=',PI
        WRITE(*,*)'A=',A
    R=SQRT(PI/A)
    PSM=B*H*H*RO
    E=75.0E+9
    PL=0.594
    WRITE(*,*)'PI.',PI
    WRITE(*,*)'E',E
    WS=(3.14*3.14/PL/PL)*SQRT(E*PI/PSM)
    WRITE(*,*)'WS=',WS/6.28

C
A1=4*RO**2*E*A+2*RO**2*PM*PL*WS**2+2**2*PM*PL*WS**2
A2=(-A1)**2
A3=32*RO**4*PM*PL*E*A*WS**2
A4=4*RO**2*PM*PL
    WRITE(*,*)'A1=',A1
    WRITE(*,*)'A2=',A2
    WRITE(*,*)'A3=',A3

X1=(A1+SQRT(A2-A3))/A4
X2=(A1-SQRT(A2-A3))/A4
WRITE (*,*)'X1=', X1
WRITE(*,*)'X2=', X2
IF(X1.GT.0.0) F1=SQRT(X1)
IF(X2.GT.0.0) F2=SQRT(X2)
WRITE(*,*) X1/6.28
C50  FORMAT(IX,'X1=?')
    WRITE(*,*) X2/6.28
C60  FORMAT(IX,'X2=?')

```

_MECHMA\$DUBO: \USERS.STUDENT.ZHOUJCI.FOR;52

```
C80      FORMAT(1X,'E2=?')
        WRITE(*,*) WS/6.28
C81      FORMAT(1X,'WS=?')
        WRITE(*,*) WS1/6.28
C85      FORMAT(1X,'WS1=?')
        STOP
        END
```

_MECHMA#DUBO:USERS.STUDENT.ZHOUJIE2.FOR;5

```
PROGRAM F2
E=75.E+9
RO=2770
E=.0125
H=.006
PSM=B*H*RO
M=5.8
PI=B*H**3/12
A=B*H
Z=.003
WRITE(*,10)
10  FORMAT(1X,'INPUT W1=')
    READ(*,*)W1
    W=W1*6.28
    A1=W**2*RO/E-4*3.14**2/.6**2
    A2=1+2/A1-M*W**2*.6/2/E/A
    A3=(-1-2*3.14**2/.6**2/A1)/A2
    A4=(3.14**2/.6**2-(-A3)/A2)/A1
    A5=A3/A2-A4+.5
    X1=(E*PI*3.14**4/.6**3)
    X2=E*A**3.14**4/.6**3
    X=X1+X2*Z**2*A5-PSM*W**2*.6
    WRITE(*,*)X
    STOP
    END
```

```
PROGRAM C4
WRITE(*,10)
10  FORMAT(1X,'INPUT X=?')
    READ(*,*) X
    WRITE(*,20)
20  FORMAT(1X,'INPUT S=?')
    READ(*,*) S
    A=.046
    B=.030
    C=.025
    D=.090
    E=.030
    F=.063
    P=.225
    XC1=A*B*(.088+B/2)+C*D*(.063+C/2)+E*F*F/2+S*P*(S/2+B+C+F)
    XC=XC1/(A*B+C*D+E*F+S*P)
    PI1=A*(B**3)/12+A*B*(B/2+C+F-XC)**2
    PI2=D*(C**3)/12+D*C*(C/2+E-XC)**2
    PI3=E*(F**3)/12+E*F*(F/2-XC)**2
    PI4=P*(S**3)/12+P*S*(B+C+F+S/2-XC)**2
    PI=7800*0.15*(PI1+PI2+PI3+PI4)
    WRITE(*,*)'XC=',XC
    WRITE(*,*)'PI=',PI
    W1=(X**4)*(75.0E+9)*(0.006**2)/12/(.6**4)/2770
    W=SQRT(W1)
    WRITE(*,*)'W=',W/6.28
    STOP
    END
```

_MECHMA4DUBO:USERS.STUDENT.ZHOUJF3.FOR;62

```
PROGRAM F3
E=75.E+9
RO=2770.
B=.0125
H=.006
PSM=B*H*RO
WRITE(*,5)
5  FORMAT(IX,'INPUT PM=')
  READ(*,*)PM
8  P1=B*H**3/12
  A=B*H
  Z=.022
  WRITE(*,10)
10 FORMAT(IX,'INPUT W1=')
  READ(*,*)W1
  W=W1*6.28
  A1=W**2*RO/E-4*3.14**2/.6**2
  A2=1+2*W**2*RO/E/A1-PM*W**2*.6/2/E/A
  A3=(-1-2*3.14**2/.6**2/A1)/A2
  A4=(3.14**2/.6**2+A3*W**2*RO/E)/A1
  A5=A3-A4+.25
  X1=(E*PI*3.14**4/.6**3)
  X2=E**3.14**4/.6**3
  X=X1+X2*Z**2*A5-PSM*W**2*.6
  WRITE(*,*)X
  STOP
  END
```